

1. Report No. FWHA/TX-05/0-1774-3		2. Government Accession No.		3. Recipient's Catalog No.	
4. Title and Subtitle Detailed Evaluation of Performance FRP Wrapped Columns and Beams in a Corrosive Environment				5. Report Date May 2004	
				6. Performing Organization Code	
7. Author(s) C. L. Shoemaker, P. N. Quiroga, D. P. Whitney, J. O. Jirsa, H. G. Wheat, and D. W. Fowler				8. Performing Organization Report No. Research Report 0-1774-3	
9. Performing Organization Name and Address Center for Transportation Research The University of Texas at Austin 3208 Red River, Suite 200 Austin, TX 78705-2650				10. Work Unit No. (TRAIS)	
				11. Contract or Grant No. Research Study 0-1774	
12. Sponsoring Agency Name and Address Texas Department of Transportation Research and Technology Transfer Office P.O. Box 5080 Austin, TX 78763-5080				13. Type of Report and Period Covered Research Report (9/97-1/00)	
				14. Sponsoring Agency Code	
15. Supplementary Notes Project conducted in cooperation with the U.S. Department of Transportation, Federal Highway Administration, and the Texas Department of Transportation.					
16. Abstract The objective of this project is to evaluate the long-term effectiveness of fiber reinforced plastic (FRP) composite wraps in preventing corrosion of reinforced concrete elements in severe environments. The experimental program was established to help determine if FRP wraps provide barriers against the transportation of chlorides into the concrete or if impermeable wraps trap chlorides and moisture beneath the wrap and thereby accelerate the corrosion process. The focus of this report is on the development of procedures for understanding data collected from 13 specimens that were removed from exposure testing and studied in detail. The specimens represent typical rectangular (beam) and cylindrical (column) elements in reinforced concrete bridges. Partially wrapped versus unwrapped elements were studied. Other parameters of interest in design and construction included: cast-in chlorides to represent specimens already exposed to a corrosive environment prior to wrapping, cracked versus uncracked elements, addition of corrosion inhibitors, and materials of repair for damage to concrete due to corrosion or to construction traffic prior to wrapping.					
17. Key Words corrosion, steel, concrete, FRP, polymer wrap, wrapping, fiber-reinforced plastics, fiber-reinforced polymers, repair, rehabilitation, encapsulation			18. Distribution Statement No restrictions. This document is available to the public through the National Technical Information Service, Springfield, Virginia 22161.		
19. Security Classif. (of report) Unclassified		20. Security Classif. (of this page) Unclassified		21. No. of pages 76	22. Price

**DETAILED EVALUATION OF PERFORMANCE FRP WRAPPED
COLUMNS AND BEAMS
IN A CORROSIVE ENVIRONMENT**

by

*C. L. Shoemaker, P. N. Quiroga, D. P. Whitney, J. O. Jirsa,
H. G. Wheat, and D. W. Fowler*

Research Report No. 0-1774-3

Research Project 0-1774

*“Effect of Wrapping Chloride Contaminated Structural Concrete
with Multiple Layers of Glass Fiber/Composites and Resin”*

conducted for the

Texas Department of Transportation

in cooperation with the

**U.S. Department of Transportation
Federal Highway Administration**

by the

**CENTER FOR TRANSPORTATION RESEARCH
BUREAU OF ENGINEERING RESEARCH
THE UNIVERSITY OF TEXAS AT AUSTIN**

June 2004

Research performed in cooperation with the Texas Department of Transportation and the U.S. Department of Transportation, Federal Highway Administration.

ACKNOWLEDGMENTS

We greatly appreciate the financial support from the Texas Department of Transportation that made this project possible. The support of the Project Director, Jon Kilgore, (SAT) and Project Coordinator, W. Cox, (BRG) is also very much appreciated. We would also like to thank monitoring committee members, R. Baker (LBB), David McDonnold (BRG), and Keith Ramsey (BRG) for their guidance on this project. The assistance of Paul Gugenheim and Delta Structural Technologies in providing materials and assistance in fabrication of specimens is gratefully acknowledged.

DISCLAIMER

The contents of this report reflect the views of the authors, who are responsible for the facts and the accuracy of the data presented herein. The contents do not necessarily reflect the view of the Federal Highway Administration or the Texas Department of Transportation. This report does not constitute a standard, specification, or regulation.

NOTICE

The United States Government and the state of Texas do not endorse products or manufacturers. Trade or manufacturers' names appear herein solely because they are considered essential to the object of this report.

**NOT INTENDED FOR CONSTRUCTION,
BIDDING, OR PERMIT PURPOSES**

James O. Jirsa, Texas P.E. No. 31360
Harovel Wheat, Texas P.E. No. 78364
David Fowler, Texas P.E. No. 27859
Research Supervisors

TABLE OF CONTENTS

1. INTRODUCTION	1
1.1 Background	1
1.2 Overview of Project 0-1774	3
1.3 Research Objectives	3
1.4 Objective of the Report	4
2. CORROSION WITHIN REINFORCED CONCRETE STRUCTURES	5
2.1 Introduction to Corrosion Damage in Reinforced Concrete	5
2.2 Microstructure and Chemistry of Concrete	5
2.3 Electrochemical Corrosion of Steel.....	7
2.4 Corrosion of Steel in Reinforced Concrete	9
3. EXPERIMENTAL PROCEDURE	11
3.1 Introduction	11
3.2 Experimental Procedure	11
3.2.1 Visual Inspections.....	12
3.2.2 Half-Cell Readings	14
3.2.3 Half-Cell Profiles and Contour Mapping.....	16
3.2.4 Chloride Content Profiles.....	17
4. PRESENTATION OF EXPERIMENTAL DATA	21
4.1 Introduction	21
4.2 Unwrapped Column Specimens	24
4.2.1 CC10 24	
4.2.2 CC11 26	
4.2.3 CC17 28	
4.2.4 CNC11	30
4.2.5 CNC20	32
4.3 Wrapped Column Specimens	34
4.3.1 CC15 34	
4.3.2 CNC6 36	
4.3.3 CNC16	38
4.3.4 CNC17	40
4.4 Unwrapped Beam Specimen	42
4.4.1 RNC2 42	
4.5 Wrapped Beam Specimens.....	44
4.5.1 RC3 44	
4.5.2 RC5 46	

4.5.3 RNC1 48

5. Discussion of Results	51
5.1 Introduction	51
5.2 Effectiveness of FRP Wrap	51
5.2.1 Comparison of Half-Cell Potentials.....	51
5.2.2 Chloride Contents	53
5.3 Effect of Other Variables	55
5.3.1 Cast-in Chlorides	55
5.3.2 Unwrapped Specimens	55
5.3.3 Repair/Repair Materials	55
5.3.4 Precracking	55
5.3.5 Corrosion Inhibitors.....	56
6. Conclusions and Recommendations	57
6.1 Summary	57
6.2 Conclusions	57
6.3 Recommendations	58
References	59
Appendix A: Test Specimen Characteristics, Status and Data	61

LIST OF FIGURES

Figure 1.1	Concrete degradation caused by rebar corrosion damage near Kingston, Ontario (Roberge 1999)	2
Figure 1.2	Highway salt usage in the United States as (from Salt Institute).....	2
Figure 2.1	Concrete degradation processes resulting form environmental effects (Roberge 1999)	6
Figure 2.2	Schematic of an electrochemical corrosion cell with separate anode and cathode regions (Chess 1998)	8
Figure 2.3	Schematic of electrochemical corrosion with continuous anode (A)/cathode(C) regions (Chess)	8
Figure 2.4	Illustration of electrochemical corrosion reactions in concrete (Roberge 1999)	9
Figure 3.1	The corrosion monitoring tank and several specimens under observation for TxDOT Project 0-1774	11
Figure 3.2	(A) Diagram of vertical labeling scheme for cylindrical specimens. (B) Lines along half-cell readings were taken for columns (36 readings @ 1 in. per line) ...	13
Figure 3.3	Diagram of horizontal labeling scheme. Section 1 corresponds with the area nearest the exposed rebar	14
Figure 3.4	Lines along half-cell readings were taken for beams.....	14
Figure 3.5	Example of reinforcing bar corrosion	14
Figure 3.6	Half-Cell potential schematic as described in ASTM C 876.....	15
Figure 3.7	Example of half-cell profile analysis along length of cylinder	16
Figure 3.8	Example of half-cell potential contours over the specimen surface	17
Figure 3.9	Example of chloride content profile.....	19
Figure 4.1	One of two large cracks located at upper-portion of CC10.	24
Figure 4.2	Data for Specimen CC10	25
Figure 4.3	Large crack on lower surface of CC11 (Typical)	26
Figure 4.4	Data for Specimen CC11	27
Figure 4.5	Data for Specimen CC17CNC11	29
Figure 4.6	Data for Specimen CNC11	31
Figure 4.7	Data for Specimen CNC20	33
Figure 4.8	Data for Specimen CC15	35
Figure 4.9	Data for Specimen CNC6	37
Figure 4.10	Data for Specimen CNC16	39

Figure 4.11	Data for Specimen CNC17	41
Figure 4.12	Data for Specimen RNC2	43
Figure 4.13	Data for Specimen RC3	45
Figure 4.14	Data for Specimen RC5	47
Figure 4.15	Data for Specimen RNC1	49
Figure 5.1	Average half-cell potential profiles for column specimens	52
Figure 5.2	Average half-cell potential profiles for beam specimens	53
Figure 5.3	Average chloride content profiles for column specimens.....	54
Figure 5.4	Average chloride contents for beam specimens.....	54

LIST OF TABLES

Table 3.1	Critical concentrations for chloride induced corrosion of steel in concrete (Klinghofer 1994)	18
Table 3.2	Recommended limits for water-soluble chloride ion content in concrete (ACI 201.2R-77)	18
Table 4.1	Construction parameters for the nine specimens selected for analysis.....	23
Table 5.1	Statistical comparison presenting percentage of data points beyond given thresholds	55

SUMMARY

The objective of this project is to evaluate the long-term effectiveness of fiber reinforced plastic (FRP) composite wraps in preventing corrosion of reinforced concrete elements in severe environments. The experimental program was established to help determine if FRP wraps provide barriers against the transportation of chlorides into the concrete or if impermeable wraps trap chlorides and moisture beneath the wrap and thereby accelerate the corrosion process. The focus of this report is on the development of procedures for understanding data collected from 13 specimens that were removed from exposure testing and studied in detail. The specimens represent typical rectangular (beam) and cylindrical (column) elements in reinforced concrete bridges. Partially wrapped versus unwrapped elements were studied. Other parameters of interest in design and construction included: cast-in chlorides to represent specimens already exposed to a corrosive environment prior to wrapping, cracked versus uncracked elements, addition of corrosion inhibitors, and materials of repair for damage to concrete due to corrosion or to construction traffic prior to wrapping.

1. INTRODUCTION

1.1 Background

Corrosion presents one of the greatest threats to our nation's infrastructure, yet for civil engineers it is also one of the least understood components of the design process. In an aggressive environment concrete structures may deteriorate in a much shorter time period than expected by both the owner and the designer. Service life issues, including corrosion, are just beginning to be major considerations in structural design.

In a paper entitled "Corrosion of Highway Bridges: Economic Impact and Control Methodologies," Yunovich and Thompson (2003) provide estimates of the cost of corrosion in the United States. A 1975 Battelle-NBS benchmark study estimated the cost of corrosion to be approximately \$70 billion/year, or 4.2% of the gross national product (GNP). In 1995 an update of the 1975 figures estimated the total cost of corrosion at \$300 billion but that number was obtained by multiplying the 1975 data by a factor based on the increase in the GNP from 1975 to 1995. In any case, the numbers reflect the seriousness of the problem.

The American Society of Civil Engineers (ASCE) conducted an extensive survey in 1998 and assigned "report card" grades to various aspects of America's infrastructure. ASCE issued a "C-" grade for the condition of bridges, estimating nearly one of every three bridges (31.4%) to be structurally deficient or functionally obsolete. An example of damage that would categorize a bridge as deficient is presented in Figure 1.1. Additionally, it was proposed that \$80 billion dollars would be necessary to eliminate the current backlog of bridge deficiencies and maintain repair levels.

Although these statistics are alarmingly high, there is encouraging data that shows a positive, albeit slow, improvement. In 1992, the Federal Highway Administration (FHWA) declared the percentage of bridge deficiencies to be 34.6%, and in 2001 ASCE (ASCE 2001) updated the grade of bridges from "C-" to "C," listing a 29% deficiency rate. FHWA's strategic plan states that by 2008 less than 25% of the nation's bridges should be classified as deficient. Federal and state funding for the rehabilitation of these deficient bridges is already very limited. Therefore, it is of critical importance to develop cost-effective and reliable solutions for preventing the progression of corrosion in existing bridge decks.

A major source of corrosion in bridge decks stems from the use of deicing salts during winter months to improve hazardous driving conditions. In the late 1960s, severe deterioration of many reinforced concrete bridge decks above the "freeze line" was noted. Despite their aggressive nature, the use of deicing salts is not likely to be discontinued. The usage of highway deicing salts from 1940-2003 is presented in Figure 1.2.



Figure 1.1 Concrete degradation caused by rebar corrosion damage near Kingston, Ontario (Roberge 1999)

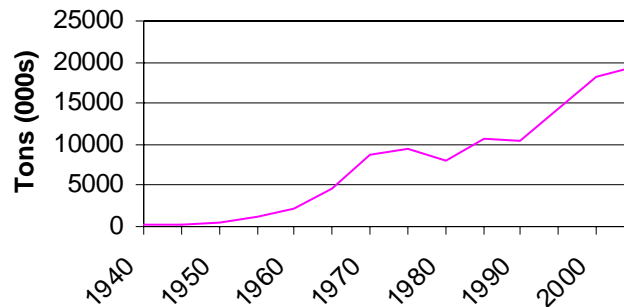


Figure 1.2 Highway salt usage in the United States (from Salt Institute)

The chloride-rich environment surrounding the use of deicing salts has prompted engineers to use several different mitigation strategies in order to protect the reinforcing steel in concrete structures. Four examples of popular methods of corrosion prevention include (1) preventing chlorides from reaching the steel surface (physical barriers at the concrete surface, coating the reinforcement, or low chloride-permeable concrete); (2) making the concrete a less corrosive environment at specific chloride levels (admixtures or inhibitors); (3) using the

reinforcement resistant to corrosion (corrosion resistant alloys, composites or clad materials); or (4) using electrochemical techniques to reduce the effect of chlorides (cathodic protection).

The use of physical barriers at the concrete surface, specifically fiber reinforced plastic (FRP) composite wraps, has become increasingly popular in combating chloride induced corrosion in concrete structures. As a non-reactive and chemically inert material, FRP should be an ideal candidate for providing a barrier against chloride intrusion at the concrete surface. However, the impervious nature of the FRP wrap could also prove harmful to the longevity of the concrete if moisture, chlorides, and oxygen are trapped and contained within the membrane.

1.2 Overview of Project 0-1774

The project entitled, “Effect of Wrapping Chloride Contaminated Structural Concrete with Multiple Layers of Glass Fiber Composites and Resin,” started in 1997. The preliminary phases of the project have been reported in CTR Research Report 0-1774-1, “Evaluation and Performance Monitoring of Corrosion Protection by Fiber-Reinforced Concrete Wrapping” (Verhulst 2001). In order to study the effects of using FRP wraps, a wide range of variables were considered such as cast-in chlorides, cracks, repairs, wet surfaces, wrap length, and presence of corrosion inhibitor. The specimens were placed in a tank and exposed to a 3.5% saline solution in order to accelerate the corrosive process. The characteristics of the initial series of specimens and their current status are shown in Appendix Table A-1. At the time the report was prepared, the experiment had not been active long enough to develop conclusions regarding the feasibility of using FRP wrapping.

After approximately three years of exposure to the aggressive environment of the soaking tank, all specimens in this study had signs of corrosion. Observations were reported in CTR Report 0-1774-2, “Effects of Wrapping Chloride Contaminated Concrete with Fiber Reinforced Plastics” (Berver 2001). The effects of using FRP as a corrosion mitigation solution were more apparent after being exposed for this length of time. Berver removed 10 columns and 4 beams from the corrosive environment and conducted autopsies that were included in Report 0-1774-2. Berver concluded that the FRP wrapping systems were effective in providing a physical barrier to the chlorides and the moisture. However, corrosion was not significantly reduced as moisture was able to enter the specimens from areas of exposed concrete and develop macrocells. In 2000, Berver constructed 17 additional specimens in which the primary variable was the effectiveness of 4 different corrosion inhibitors. Those specimens are listed in Appendix Table A-4. The construction details were included in Report 0-1774-2.

1.3 Research Objectives

The objective for TxDOT Project 0-1774 is to determine the long-term effectiveness of FRP composite wraps in extending the life of reinforced concrete structures. The challenge is to establish a comprehensive database so that the influence of a wide range of variables included in the test program can be determined.

1.4 Objective of the Report

The main focus of Project 0-1774 is the development of an understanding of the long-term effects of fiber reinforced plastic (FRP) composite wraps in preventing corrosion. The specific goal of this thesis is to examine the behavior of specimens that represent the support structure typical of reinforced concrete bridges. A key feature of the project is to ascertain whether FRP wraps provide effective barriers against the transportation of chlorides into the concrete and to assess the likelihood that the impermeable nature of the wraps may trap chlorides and moisture beneath the wrap and accelerate the corrosive process.

The results of a detailed examination of 9 column and 4 beam specimens that were removed from the exposure tank will be presented. Half-cell potential readings were taken at small intervals over the entire surface of specimens after the FRP wrapping was removed. Extensive chloride-content sampling was carried out to supplement the half-cell potential readings. Chloride contents were compared with half-cell potential readings and with visual observations of the condition of reinforcing bars that were extracted from the concrete as the final step of the “autopsy” process.

In addition the details of all the specimens fabricated and subjected to a corrosive environment in the project are summarized in Appendix A concluding:

- Characteristics and status of specimens (Table A-1)
- Chronological record of half-cell readings of specimens (Table A-2)
- Half-cell and chloride content readings for specimens removed from exposure testing (Table A-3)
- Characteristics and chronological record of half-cell readings of specimens with different corrosion inhibitors (Table A-4)

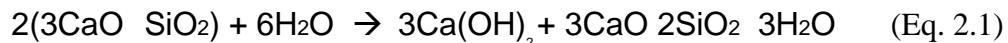
2. CORROSION WITHIN REINFORCED CONCRETE STRUCTURES

2.1 Introduction to Corrosion Damage in Reinforced Concrete

The manner in which the mechanical and chemical properties of concrete serve to both protect and expedite the corrosion of reinforcing steel will be discussed. Concrete is a composite material complex in microstructure and chemical reactivity. In order to understand how reinforcing steel corrodes in this environment, this microstructure must be understood. Additionally, the electrochemical corrosion process for steel will be examined considering the effects of a surrounding cement paste matrix and chloride ion migration.

2.2 Microstructure and Chemistry of Concrete

A composite material is defined as being comprised of two or more separate substances and one that exhibits behavior influenced by, yet unique from, the constituent materials. Concrete is a complex composite material made up of cement clinker, water, fine aggregate, coarse aggregate, and certain special additives. The ground cement clinker, typically portland cement, is mixed with water to form the cement paste. The cement paste matrix surrounds the coarse and fine aggregate and serves to bind the material together. An example of the complex hydration reaction that forms the cement paste is:



A fibrous network of voids and water-filled spaces characterizes the microstructure of the cement mortar. These pores that are formed due to excess water in the concrete mix are known as capillary pores. Additionally, entrained air adds to the non-homogeneity of concrete and creates air voids within the cement paste. This porous and permeable microstructure presents ample opportunity for the transportation of corrosive agents such as chlorides to the surface of reinforcing steel.

The exact impact of this porosity on the corrosion of reinforcing steel is an issue of debate among industry experts (Roberge 1999). One approach is represented by Mehta's holistic model of concrete degradation. Mehta challenged the prevailing notions that emphasize porosity and permeability. Traditionally, it was believed that lower strength concrete mix designs and the subsequent high water-to-cement ratio resulted in less durable structures. With higher water-to-cement ratios, a microstructure with higher porosity would develop.

Mehta argued that the development of a network of connected microcracks and other defects was a more serious factor in the development of corrosion. Concrete manufactured under high quality standards was initially considered to be impermeable, and interior pores and microcracks did not form interconnected paths extending to the exterior surface. However, the effects of continuous cyclic loading and environmental weathering result in the development and propagation of interconnected cracks. This network of defects, compounded by the inherent porosity, provides a route for transporting corrosive agents to the surface of the reinforcing steel beneath the layer of protective cover. A schematic of Mehta's model of environmental degradation is presented in Figure 2.1.

Another approach on the influence of the microstructure on corrosion, as stated by Chess (Chess 1998), is based on the inherent porosity of concrete. It is suggested that if there is a concentration gradient, then at some time a sufficient quantity of aggressive ions will be passed through the concrete to initiate corrosion.

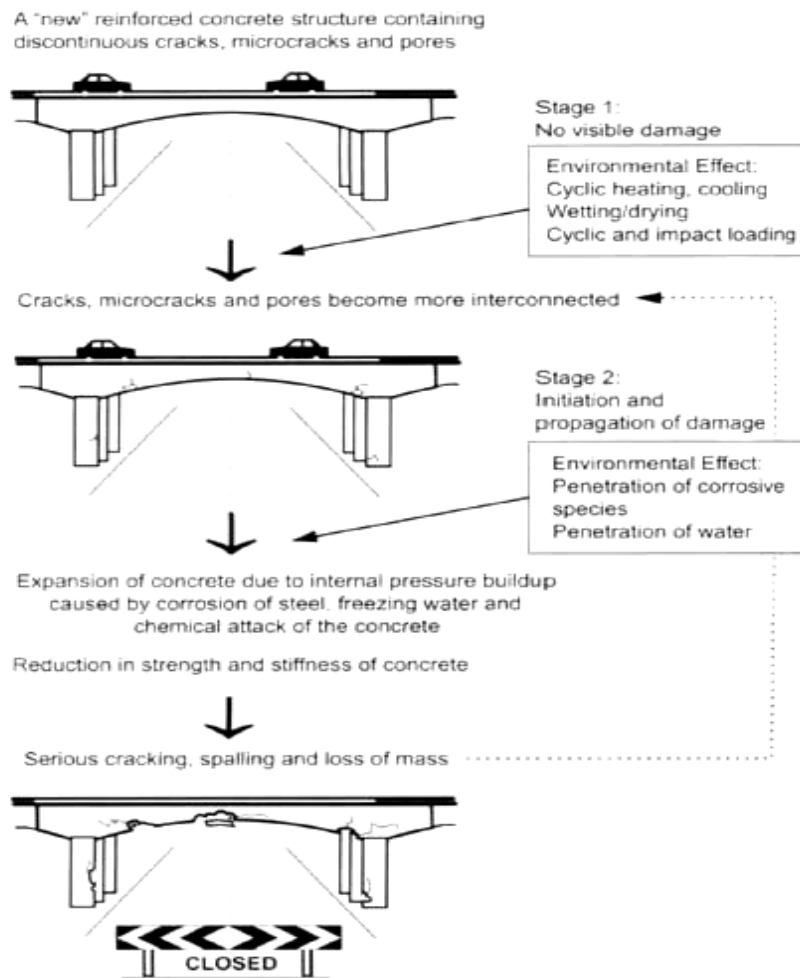


Figure 2.1 Concrete degradation processes resulting from environmental effects (from Roberge 1999)

Rather than assume concrete is initially impermeable, as Mehta does, this philosophy relies on the factor of time and the inevitability of enough contaminants migrating to the steel to cause corrosion. Although these two theories emphasize the importance of either cracks or porosity to the transportation of corrosive catalysts, both are based on the fact that passage of time is an important and difficult variable to quantify in the corrosion of reinforcing steel.

2.3 Electrochemical Corrosion of Steel

A metal is manufactured by transforming an ore in its stable state to a metallic material, which is not stable under most conditions found in practice. Therefore, when metals are exposed to the weather they naturally seek to return to a more stable state as an ore. In this process the metallic iron is converted to ferrous/ferric compounds such as oxides and hydroxides (commonly known as rust).

The corrosive process can be divided into two categories: electrochemical corrosion, which takes place via electrode reactions, usually in a moist environment (corrosion in aqueous solutions, atmospheric corrosion under the influence of moist films on the surface, and corrosion aided by moisture is included here) and chemical corrosion, which takes place under the influence of dry gases (for example high temperature oxidation) or water-free organic liquids (Mattsson 1989). For the purpose of this investigation, only electrochemical corrosion will be examined.

An overall electrochemical reaction consists of two individual reactions: oxidation and reduction. The oxidation reaction takes place when a metal atom loses or gives up an electron. The location where oxidation takes place is called the anode, and consequently oxidation is sometimes called an anodic reaction. The electrons generated from each metal atom that is oxidized must be transferred to and become part of another chemical species in what is termed a reduction reaction. Similarly, the location where reduction occurs is called the cathode and may also be known as a cathodic reaction. Both reactions are necessary in an electrochemical reaction, and thus the individual reactions are termed half-cell reactions.

It is important to note that there can be no net electrical charge accumulation from the electrons and ions. The total rate of oxidation must equal the total rate of reduction, or all electrons generated through oxidation must be consumed by reduction (Callister 2000).

An example of a common electrochemical reaction is presented in Figure 2.2. This corrosion system, also known as an electrochemical cell, is made up of separate and distinguishable anode and cathode regions. An example of such a system is an aluminum sheet with brass screws, where the aluminum constitutes the anode and the brass the cathode (Mattsson 1989).

Another example of an electrochemical reaction is presented in Figure 2.3. Here, the difference from the preceding example is that the corrosion cell would exist without distinguishable anode and cathode surfaces. Part of the metal surface forms the anode and part forms the cathode. In this case, the corrosion occurs at all the anode points giving the appearance of general or uniform corrosion.

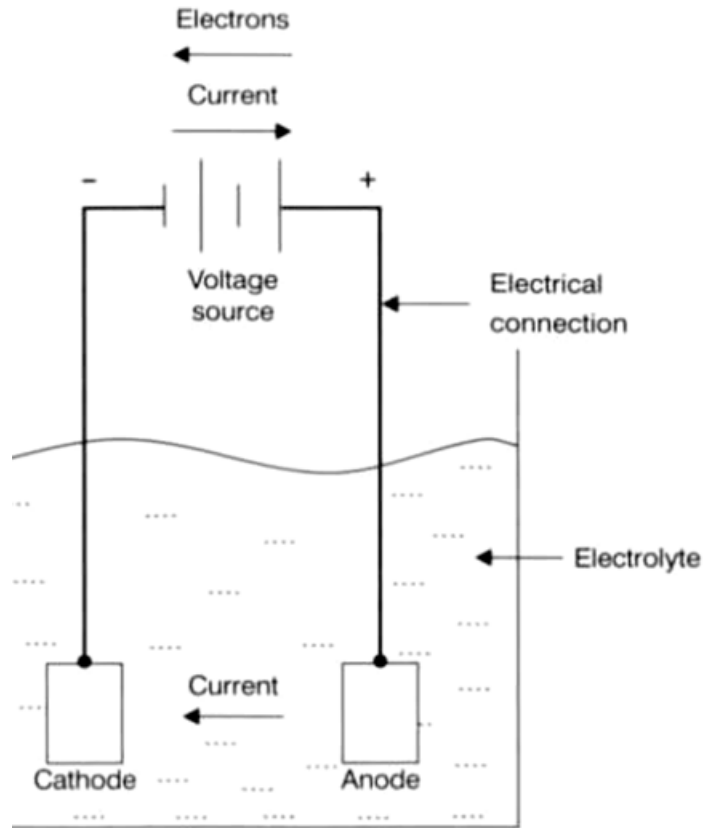


Figure 2.2 Schematic of an electrochemical corrosion cell with separate anode and cathode regions (Chess 1998)

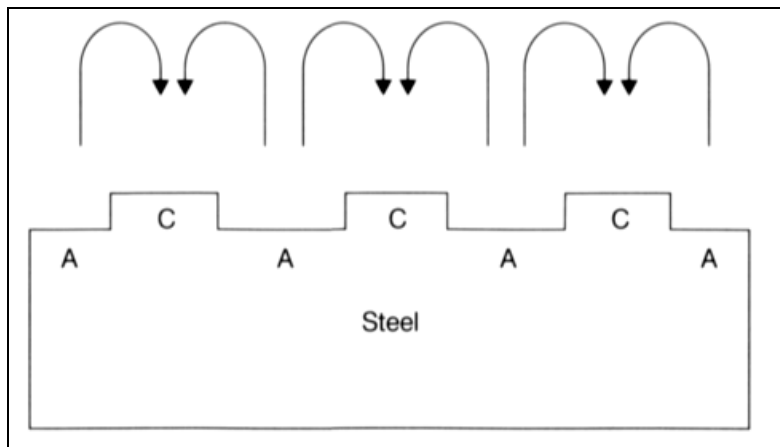


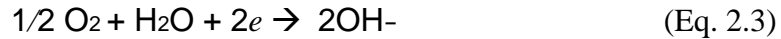
Figure 2.3 Schematic of electrochemical corrosion with continuous anode (A)/cathode (C) regions (Chess 1998)

2.4 Corrosion of Steel in Reinforced Concrete

One of the most common mechanisms of reinforcing steel corrosion damage in concrete is localized breakdown of the passive film by chloride ions. Chloride is readily available in common sources such as highway deicing salts and marine environments, and propagates rather easily through the permeable microstructure of concrete. In a chloride-free environment, the oxidation reaction of iron,



is balanced by the reduction reaction,



Oxygen molecules are transported to the steel surface via porosity within the concrete microstructure and networked cracks within the cover material. The Fe^{2+} ions produced at the anodes combine with the OH^- ions from the cathodic reaction, producing a stable passive film. This procedure is outlined in Figure 2.4.

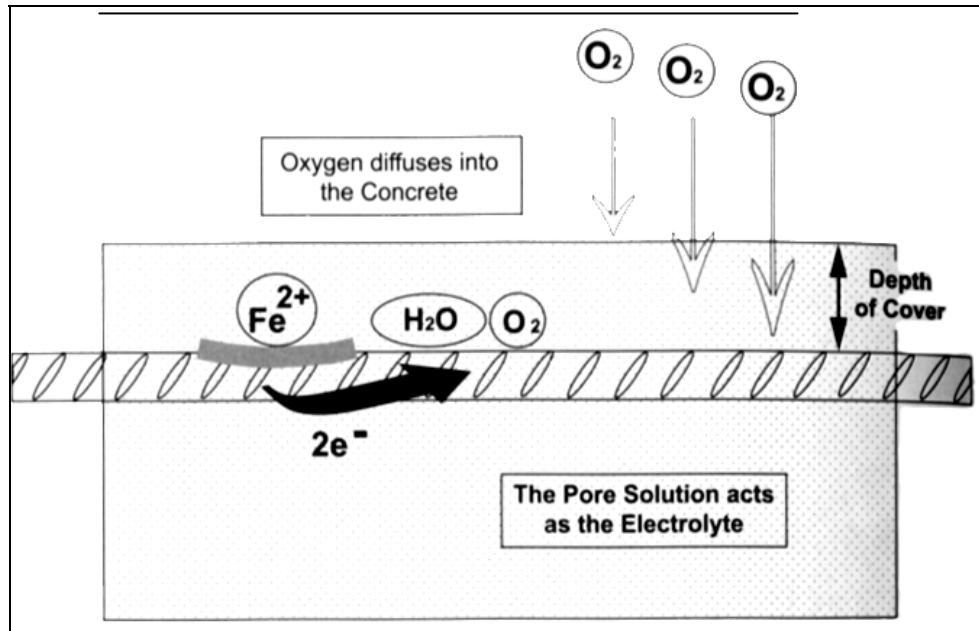


Figure 2.4 Illustration of electrochemical corrosion reactions in concrete (Roberge 1999)

Chloride ions, having the same charge as OH^- ions, compete with the hydroxyl ions to combine with Fe^{2+} cations. With increasing quantities of soluble chlorides present at the iron-cement paste interface, chloride ions appear to be a specific destroyer of the protective oxide film (Chess 1998).

These harmful chloride ions can either originate from the concrete mix constituents or diffuse into the concrete from the surrounding environment. An example of chloride in the "as-manufactured" concrete is the additive calcium chloride, which accelerates hardening

at low temperatures. Another source of chloride is the use of seawater or aggregate that has been exposed to saline water (i.e. beach sand).

The most common source of environmental chloride contamination occurs from the application of deicing salts to highways and bridges in cold-weather locations.

Chloride ions are not the only limiting factor in the corrosion process of steel in concrete. Another essential factor for the corrosion of steel in concrete is the presence of oxygen at the steel to cement paste interface (Chess 1998). As shown in the reaction Eq. 2.3, oxygen is required in addition to chlorides. Also, the concrete composition itself has a bearing on the amount of corrosion damage that occurs at a chloride concentration. One example presented by Chess, is that hardened concrete appears to have a lower chloride tolerance level than concrete that is contaminated during mixing. However, it is important to note that although cement composition and type can affect corrosion, this effect is relatively small compared to the concrete quality, cover over the steel, and concrete consolidation.

3. EXPERIMENTAL PROCEDURE

3.1 Introduction

In this chapter the challenges involved with analyzing the experimental data will be discussed. The approach for quantifying the results and interpreting various trends and correlations will be outlined.

It was important to develop a test procedure that provided a means for comparing results in a specific and measurable manner. The evaluation process was complicated by the fact that a large number of test specimens, and a large number of variables were included in the test program.

3.2 Experimental Procedure

The laboratory specimens were placed in a specially designed exposure tank that was designed to provide a corrosive environment similar to that in which structural elements of a highway might be exposed. Also, the conditions were intended to be especially severe in order to accelerate the corrosion process.

The columns were arranged in a series of rows in the base of the tank, as shown in Figure 3.1. A 3.5% saline solution was introduced to the tank on a one-week cycle. During the wet period, the water level reached the lower one-foot of the columns. Following the one-week wet cycle, the tank was drained and remained dry for another two-week period.



Figure 3.1 The corrosion monitoring tank and several specimens under observation for TxDOT Project 0-1774

As described in preceding sections, the sheer volume of specimens and experimental parameters involved with this project necessitates having a well-defined and structured procedure for quantifying the experimental data. By developing a systematic method for analyzing the specimens, the material presented in this report is intended to serve as a template for systematically evaluating data over the remainder of the project duration.

The basic outline for collecting data includes four distinct experimental methods: (1) visual inspections, (2) half-cell readings, (3) half-cell profiles and countour maps, and (4) chloride content profiles, as explained below.

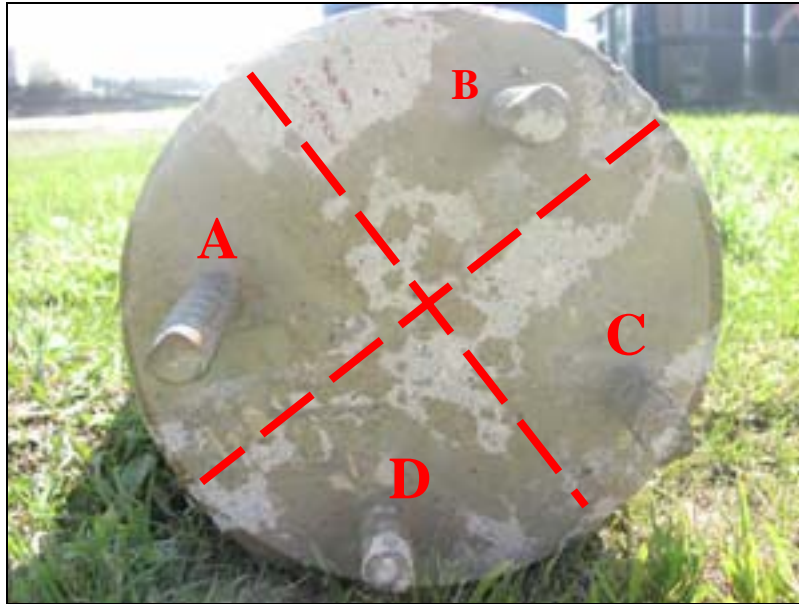
3.2.1 Visual Inspections

The first phase of the data collection and analysis involved extensive visual inspections on each specimen following its removal from the exposure tank. The examination process was divided into two subsections: the exterior and the interior of each specimen. In addition to photographing each specimen, detailed written descriptions of important characteristics were collected.

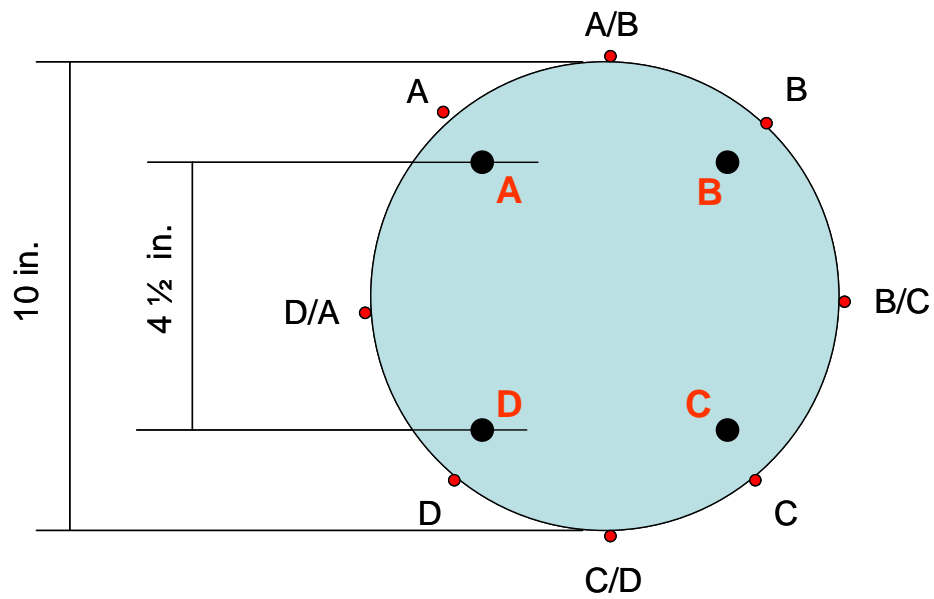
Initial inspections were conducted on the exterior of each specimen. First, the observations were recorded without the removal of any FRP wrap or other repair materials. The surface was inspected for cracking or corrosion staining.

The same procedure was conducted following the removal of the FRP wrap. Visual observations were carefully catalogued so that comparisons and other correlations could be easily drawn between the various levels of inspection. A grid of the surface of each specimen was used as shown in Figures 3.2 and 3.3. Cylindrical specimens were divided into four equal segments labeled “A” through “D.” Additionally, the cylinder was cut into three regions down the height, subdivided for each 12-inch section and labeled “1” through “3.” Rectangular specimens had the same labels for the side, top, and bottom sections, as shown in Figure 3.4.

Finally, visual observations of the reinforcing steel after removal of the concrete were recorded. Of critical importance was cataloguing the locations where corrosion took place on both the main (longitudinal) bar and the transverse reinforcement. In addition to visual reports describing the corrosion, a graphical approach was utilized to simplify comparisons between specimens. This graphical schematic is presented in Figure 3.5. A picture of the exposed rebar shows the original element, and locations where corrosion was observed are delineated to make it easier for the reader to visually identify locations of corrosion activity.



(A)



(B)

Figure 3.2 (A) Diagram of vertical labeling scheme for cylindrical specimens. (B) Lines along half-cell readings were taken for columns (36 readings @ 1 in. per line)

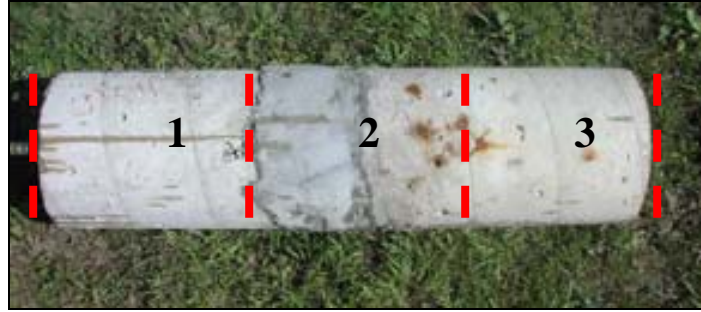


Figure 3.3 Diagram of horizontal labeling scheme
Section 1 corresponds with the area nearest the exposed rebar

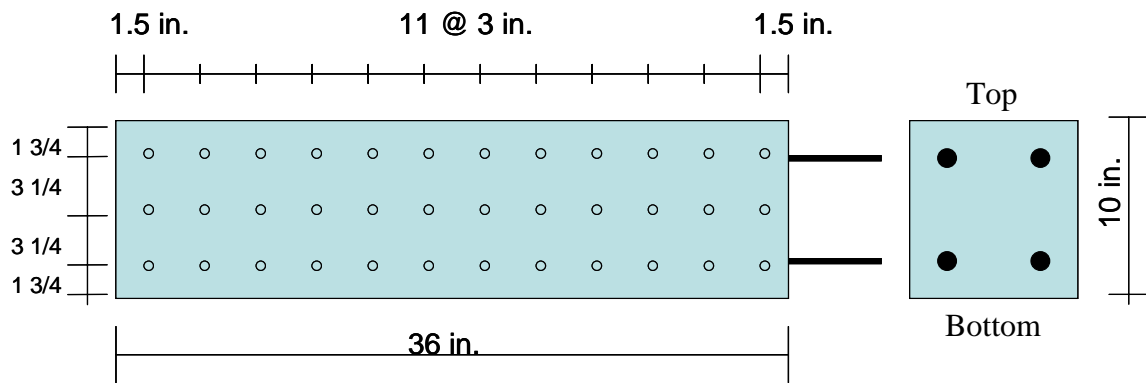


Figure 3.4 Lines along half-cell readings were taken for beams



Figure 3.5 Example of reinforcing bar corrosion

3.2.2 Half-Cell Readings

The second phase in processing data involved analysis of half-cell readings taken on the specimens throughout their duration in the exposure tank. The half-cell readings are based on the electrochemical properties of the corrosion reactions and provide important data for analyzing the extent of corrosive activity using a nondestructive technique. In Project 0-1774, the half-cell potential method for determining the likelihood of corrosion was utilized in two separate procedures. The readings were used to develop a “time-history” of potential at a given location over the time the specimens were exposed to a corrosive environment. In addition, readings were used to produce profiles of corrosion over the surface of the entire specimen when the specimens were removed from exposure testing and studied. Profiling is described in Section 3.2.4. Half-cell values were recorded at a single location on each specimen over its “lifetime” in the exposure tank. The exposure was cycled in two-week intervals. One half-cell reading was recorded upon the completion of the “wet” cycle, and another reading was recorded following the “dry” cycle. The time-

history was used to predict the likelihood of corrosive activity. By comparing the readings from different specimens it became evident which specimens had better protective properties and which elements were more prone to corrosion.

During the electrochemical corrosion process there are two individual chemical reactions that occur. The anodic (i.e. corrosion) reaction takes place when atoms of one material lose electrons into a solution as positively charged ions. The cathodic reaction involves the combination of electrons with positive ions in the solution to produce an atom that deposits on the electrode. The net result of the two reactions is an increase in positive ions in the solution containing the anode and a depletion of positive ions in the solution containing the cathode. To sustain the half-cell reactions, there must be a connection between the two solutions so that electrical neutrality is maintained (Carino 1999).

The ease with which the half-cell reactions occur is governed by their half-cell potentials measured in volts (Carino 1999). These potentials affect the tendency of the anode to corrode when the external circuit is completed. Thus, the more negative the potential, the greater the propensity for the metal to give up electrons. As defined above, the anodic reaction represents the loss of electrons. Therefore, measuring the voltage presents a way of predicting the tendency for corrosion at a given point on the metal.

The standard test method for measuring this potential is given in ASTM C 876 and is presented in Figure 3.6. This setup includes a copper-copper sulfate half-cell, connecting wires, and a high-impedance voltmeter. The positive terminal is attached to the reinforcement and the negative terminal is attached to the half-cell.

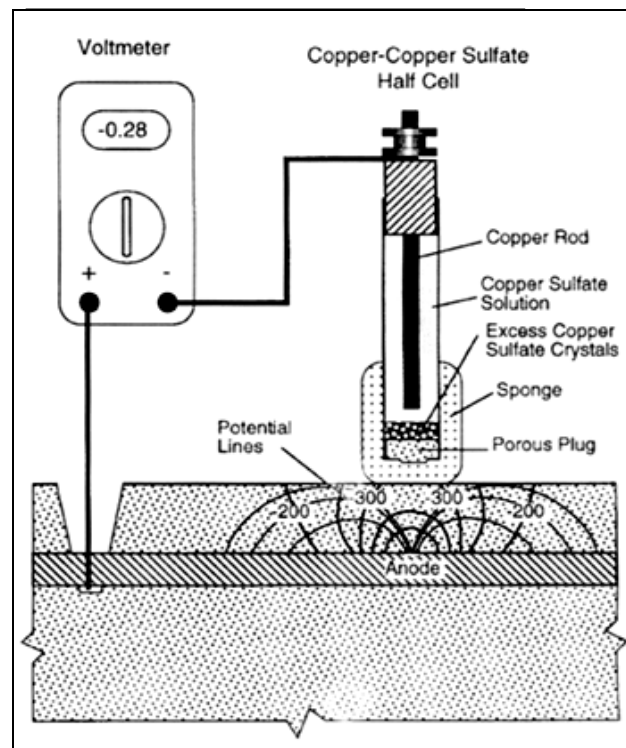


Figure 3.6 Half-Cell potential schematic as described in ASTM C 876

When corrosion is occurring, free electrons in the bar would flow from the bar to the half-cell. This layout of this circuit is such that the voltmeter indicates negative voltage. The more negative the voltage, the higher the probability corrosion is taking place below the half-cell probe.

Van Deveer (1975) found that there was a 90% probability of corrosion in regions where the potential was more negative than -350 mV with respect to a copper/copper sulphate reference electrode and a 5% probability where the potential was less negative than -200 mV. It should be noted that these criteria serve only as an estimate and are not an absolute indicator of corrosion.

3.2.3 Half-Cell Profiles and Contour Mapping

In addition to generating a time-history of half-cell values for each specimen in the exposure tank, potential readings were also taken over the surface of a specimen. Once the FRP wraps were removed it was possible to find the half-cell potential values at any location. Using these values, it was possible to create profile and contour maps of potential and to visualize areas where corrosion is most likely.

The reference probe was placed at one-inch intervals and the resulting potentials were plotted to generate a profile of potential readings along the entire length of reinforcing steel, such as that presented in Figure 3.7.

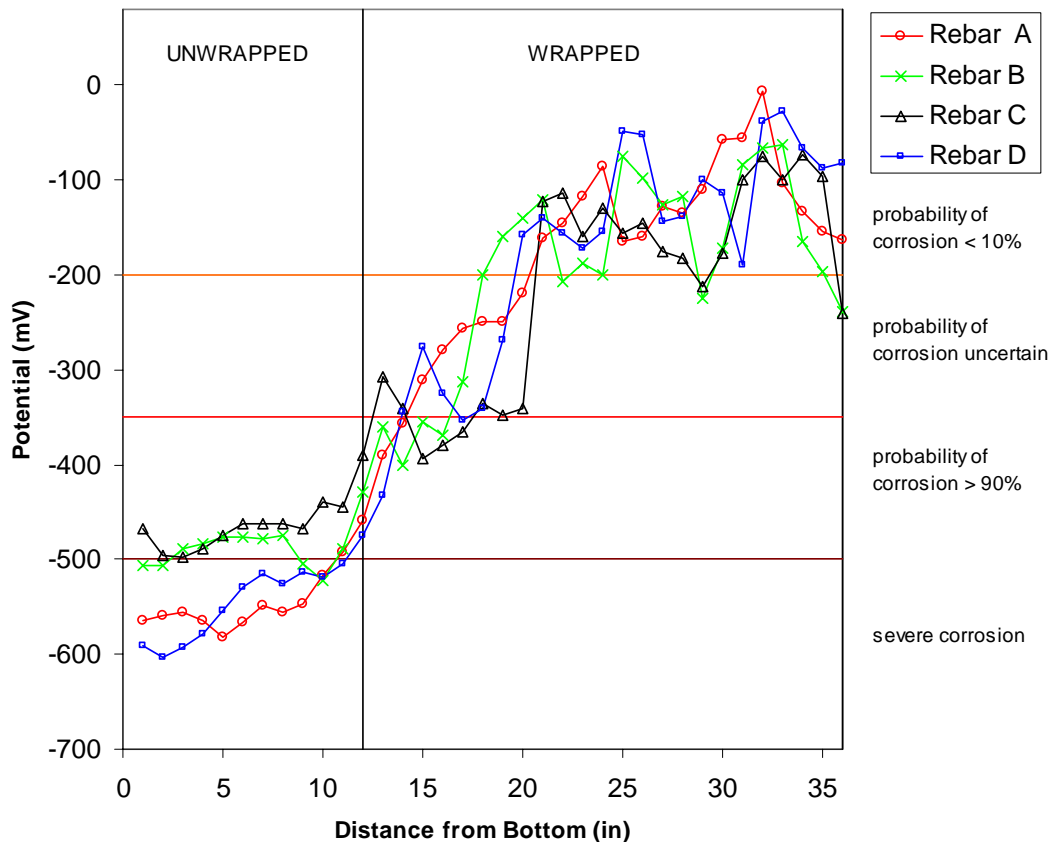


Figure 3.7 Example of half-cell profile analysis along length of cylinder

The profile created a visual representation of the location of probable corrosive activity and proved to be a useful tool in gauging the performance of each specimen.

To provide data for plotting contours of half-cell readings over the surface of the specimens, another series of readings were taken as a line midway between the longitudinal bars. All the half-cell potential readings were combined (readings at 8 points around the circumference of the specimen at 1-inch intervals over the 36-inch height or length of the specimen for a total of 288 readings) and used in a statistical analysis program MATLAB to generate equipotential contour maps for the surface of each specimen. By connecting points where the potential is equal, the graph indicated where corrosion was most likely taking place (Fig. 3.8).

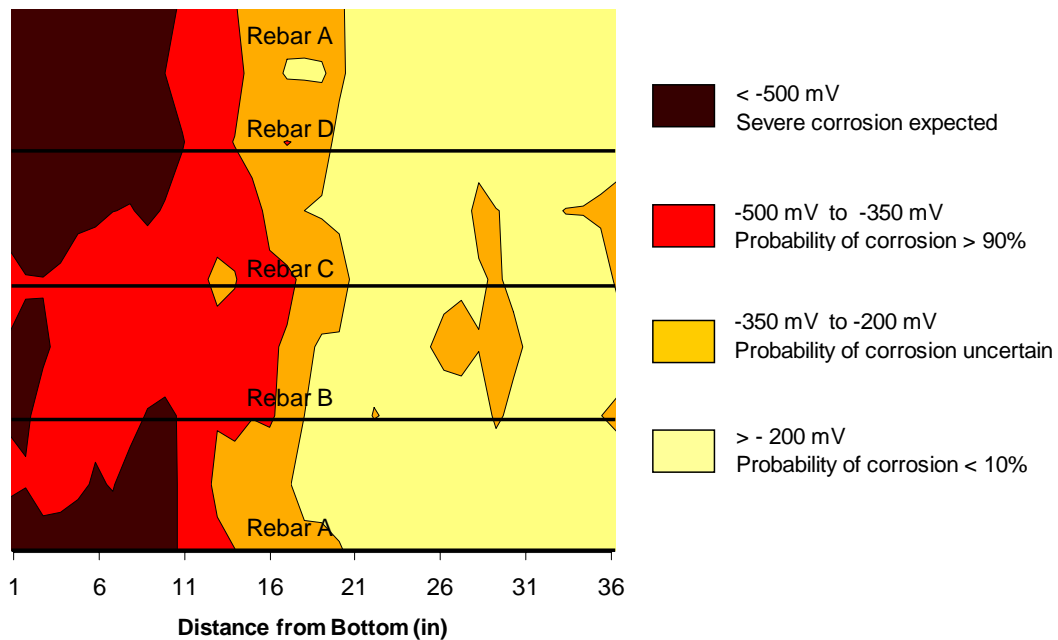


Figure 3.8 Example of half-cell potential contours over the specimen surface

3.2.4 Chloride Content Profiles

The chloride content at selected locations and depths along the surface of each specimen was determined to provide a separate means of assessing the likelihood of corrosion. Chess suggests that there is a threshold concentration of chloride ions that must be exceeded in an oxygen rich environment before there is a significant level of steel reinforcement corrosion occurring. Some of the suggested values for this level are given in Tables 3.1 and 3.2. These values are determined calculated with respect to concentrations to weight of concrete or to weight of cement, respectively.

A standard estimation of the critical chloride threshold is one pound of chloride per cubic yard of concrete and is equivalent to about 0.03% chlorides per weight of concrete and 0.22% chlorides per weight of cement. For this report, values of chloride concentrations were calculated as a percent of the weight of concrete and the critical threshold for chloride-induced corrosion was assumed to be 0.03% (Berver 2001).

Table 3.1 Critical concentrations for chloride induced corrosion of steel in concrete (Klinghofer 1994)

Authority	Cl (%) by Weight of Concrete
Wiegler	0.40
BS CP11 1979	0.35
Clear	0.20
Knofel	0.20
ACI Committee 201	0.15
Vassie	0.10

Table 3.2 Recommended limits for water-soluble chloride ion content in concrete (ACI 201.2R-77)

Category of Concrete Service	Maximum Water-Soluble Chloride Ion Content Percent by Weight of Cement
Prestressed concrete	0.06
Conventionally reinforced concrete in a moist environment and exposed to chloride	0.10
Conventionally reinforced concrete in a moist environment but not exposed to chloride	0.15

The concrete samples were drilled and tested according to the procedure outlined in ASTM C 1152. The sampling locations for the cylindrical specimens examined in this project were 6 in., 16 in., 26 in., and 36 in. from the base of the specimen. The depths at which the samples were collected were from 1/2 to 3/4 in., 1 1/4 to 1 3/4 in., and 2 1/4 to 2 3/4 in. Similar to the half-cell profiles outlined in the preceding section, generating a visual representation of the chloride content across the height and depth provided valuable information on corrosion mitigation. An example of the type of profile generated by gathering the chloride concentrations is presented in Figure 3.9.

The profile of chloride content is helpful in understanding the extent of corrosion by:

- (1) providing a graphical representation of the likelihood of chloride induced corrosion; and
- (2) serving as a comparison with the other profiles generated by half-cell potential mapping.

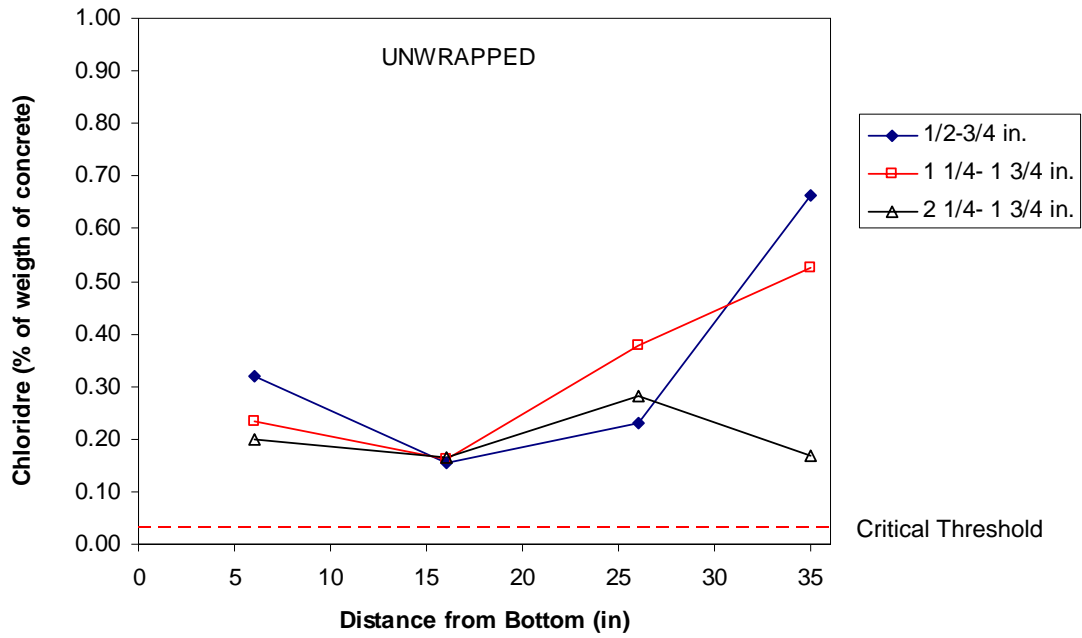


Figure 3.9 Example of chloride content profile

4. PRESENTATION OF EXPERIMENTAL DATA

4.1 Introduction

Nine cylindrical (column) and four rectangular (beam or pier cap) specimens were removed from observation in the exposure tank for a detailed and thorough examination. In order to develop a complete understanding of the effectiveness of the construction parameters, specimens were selected incorporating a broad range of experimental variables. A complete listing of the specimens and their respective construction parameters is presented in Table 4.1.

The emphasis of the discussions in this chapter is developing an understanding of how effectiveness of the FRP wrap in preventing corrosion activity. For this reason, the results are divided into two main sections: unwrapped versus wrapped. After comparing the behavior of the wrapped and unwrapped specimens, the other parameters are analyzed.

The first portion of each section outlines information gathered during the visual inspection of each specimen. This includes both inspection of the exterior as well as one bar extracted from each specimen. A photograph of the rebar is presented for each specimen and areas of corrosion are highlighted.

The graphical presentation of half-cell readings across the surface of the concrete cylinders and beams is a very powerful tool in understanding the location of corrosion activity. Linear profiles obtained by measuring the half-cell potential above the embedded reinforcing bars are used to plot contours of the potential across the entire surface in two-dimensions to create a more effective picture of where corrosive activity is most likely.

A few important notes should be reemphasized before examining these graphs. First, the more negative the electrical potential, the more likely there is corrosive activity directly below or nearby on the reinforcing steel. Secondly, on each graph there are two ledger lines that indicate corrosion probability thresholds. Half-cell values more negative than -350 mV represent a probability of corrosion higher than 90% (Van Deveer 1975). Values more negative than -500 mV are a strong indication of corrosion and cracking within the concrete (Berver 2001).

The final portion of the experimental analysis involved measuring the chloride content at various locations and depths across the height of each cylinder. The chloride content is important because it will reveal critical information on the permeability of the concrete and other effects of the FRP wrap in either preventing or trapping the transportation of salts.

Each graph shows the chloride content as a percentage of the total weight of concrete. Also on each graph is a critical chloride threshold of 0.03 %, above which corrosion is likely (Berver 2001).

Table 4.1 Construction parameters for the nine specimens selected for analysis

Specimen	Wrap	Resin	Curing Agent	Surface	Crack Condition	Repair Material	Corrosion Inhibitor
Unwrapped Column Specimens							
CC10	None	None	None	Dry	Uncracked	None	Ferrogard
CC11	None	None	None	Dry	Uncracked	None	None
CC17	None	None	None	Dry	Uncracked	LMC	None
CNC11	None	None	None	Dry	Uncracked	LMC/Patch	None
CNC20	None	None	None	Dry	Uncracked	None	None
Wrapped Column Specimens							
CC15	Generic 24-in.	862	3090	Dry	Cracked	None	Ferrogard
CNC6	Generic 24-in.	Vinyl Ester	411	Wet	Cracked	Patch	None
CNC16	Delta 24-in.	Delta System	Delta System	Dry	Uncracked	LMC	None
CNC17	Delta 24-in.	Delta System	Delta System	Dry	Uncracked	EG	None
Unwrapped Beam Specimens							
RNC2	None	None	None	Dry	Uncracked	None	None
Wrapped Beam Specimens							
RC3	Delta 24	Delta System	Delta System	Dry	Cracked	None	None
RC5	Delta 27	Delta System	Delta System	Dry	Uncracked	LMC	None
RNC1	Delta 24	Delta System	Delta System	Dry	Uncracked	None	None

4.2 Unwrapped Column Specimens

4.2.1 CC10

The construction variables for CC10 are listed below.

Wrap	None
Resin	None
Curing Agent	None
Surface	Dry
Crack Condition	Uncracked
Repair Material	None
Corrosion Inhibitor	Sika

The concrete mix contained the corrosion inhibitor Sika Ferrogard in addition to cast-in chlorides.

This specimen was characterized by two large cracks (Figure 4.1), both of which extended from the top of the cylinder downwards. One crack was located between rebars A and B (See Figure 3.2) and extended two inches from the top to eleven inches from the bottom. The second large crack was located between rebars C and D and extended three inches from the top down to the bottom.



Figure 4.1 One of two large cracks located at upper-portion of CC10.

With these extensive and wide cracks, it was not surprising that corrosion was visible across the entire length of the extracted rebar. The visual evidence of corrosion activity along the entire bar length (Figure 4.2a) was corroborated by both the half-cell and the chloride content data.

In Figure 4.2b, most of the data is located beyond the threshold of 90% probability of corrosion. Furthermore, the area between 28 inches and 36 inches from the bottom indicates that severe corrosion is likely. Upon closer inspection of the photograph of the rebar, areas of intense discoloration could be easily identified in this region of heavy corrosion. The half-cell contour plot for CC10 (Fig. 4.2c) indicates a strong likelihood of corrosion across most of the specimen, with the highest concentrations at the top.

The chloride content variation presented in Figure 4.2d, provide additional corroboration of the visual and analytical observations. The highest concentrations of chlorides are in the section of the cylinder where the damage was most severe.

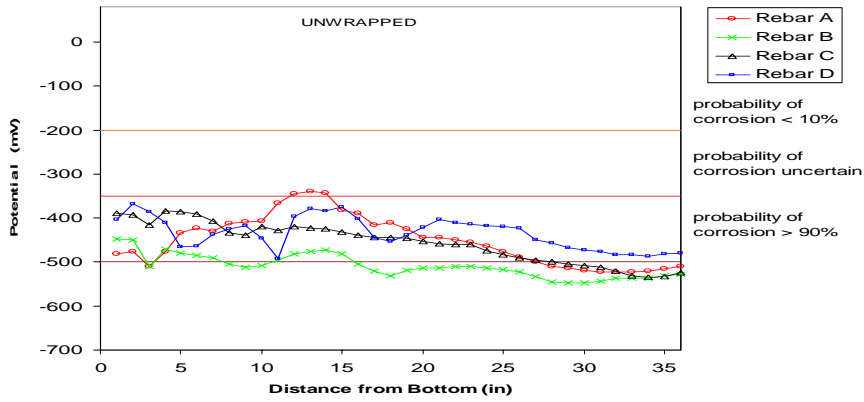
CYLINDER CC10

Wrap	None
Resin	None
Curing Agent	None
Surface	Dry
Crack Condition	Uncracked
Repair Material	None
Corrosion Inhibitor	Sika

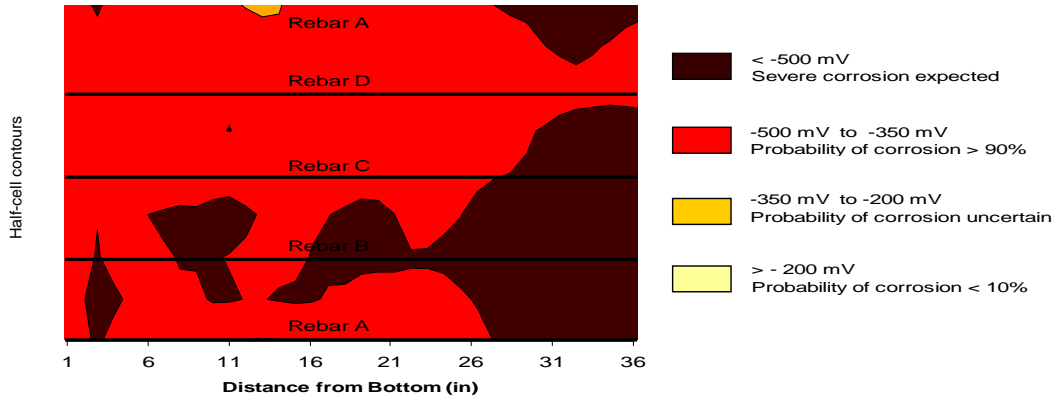


Corroded zones

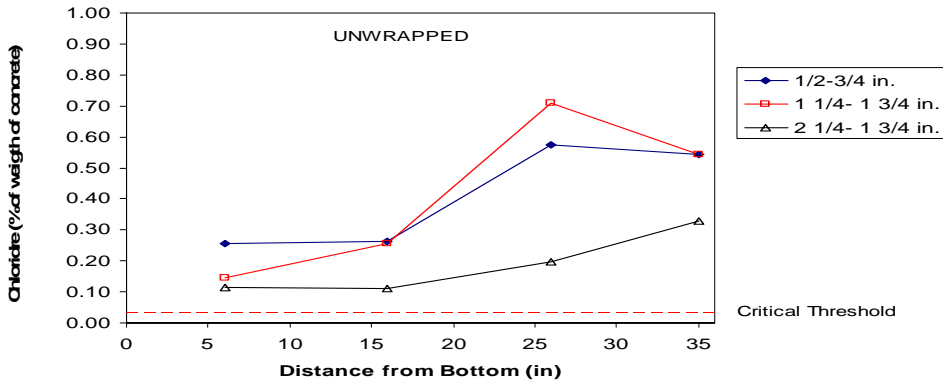
a) Corrosion activity



b) Half-cell potential profiles



c) Half-cell potential contours



d) Chloride content profiles

Figure 4.2 Data for Specimen CC10

4.2.2 CC11

Column CC11 is a control specimen for this project constructed with no inhibitors, additives, or other protective features. The only modified property in this cylinder is the addition of cast-in chlorides.

Wrap	None
Resin	None
Curing Agent	None
Surface	Dry
Crack Condition	Uncracked
Repair Material	None
Corrosion Inhibitor	None

Corrosion stains and related cracking are primarily located in the lower half of specimen CC11. There are large, open cracks (Fig. 4.3) located above rebars B, C, and D along the lower half to two-thirds of the height.

The regions of corrosion activity in the lower two-thirds of the element, as shown in Figure 4.4a. The highest activity appeared to be in the bottom five inches and from 15 inches to 24 inches from the bottom.



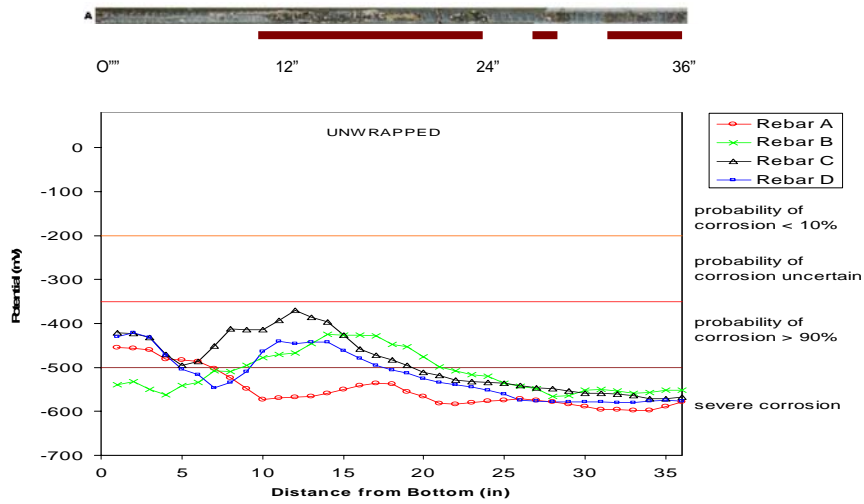
Figure 4.3 Large crack on lower surface of CC11 (Typical)

The half-cell profile and contour plots indicate that corrosion was likely over the entire length of the specimen (Figs. 4.4b and c). Potential readings were beyond the 90% probability threshold. Interestingly, the region with the highest values is located in the upper-portion of this specimen, although visual evidence of corrosion on the exposed rebar does not indicate significant corrosion in this area. Further study of the remaining reinforcing elements will be necessary in order to confirm whether or not corrosion is taking place in the region near the top of the cylinder.

The chloride content profile for this unwrapped specimen (Fig. 4.4d) follows the same peculiar trend as the one witnessed in CC10. Here, all samples reflect concentrations of chloride above the 0.03% threshold and indicate a strong probability of corrosive activity.

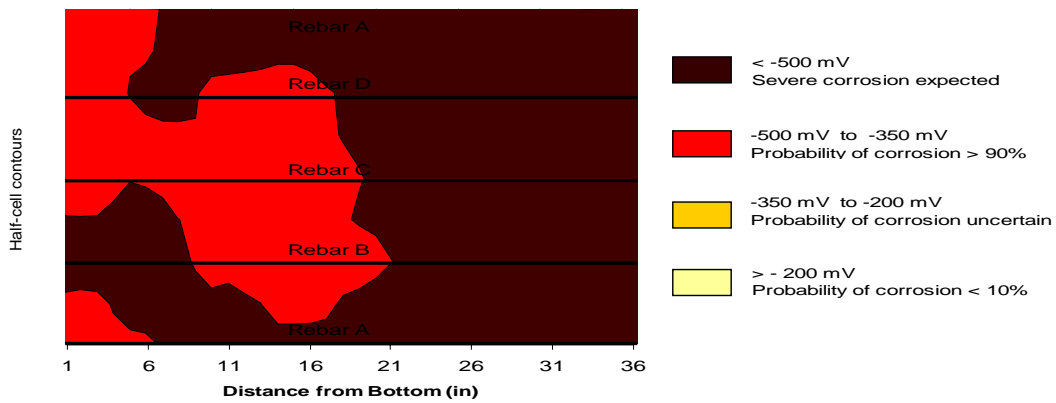
CYLINDER CC11

Wrap	None
Resin	None
Curing Agent	None
Surface	Dry
Crack Condition	Uncracked
Repair Material	None
Corrosion Inhibitor	None

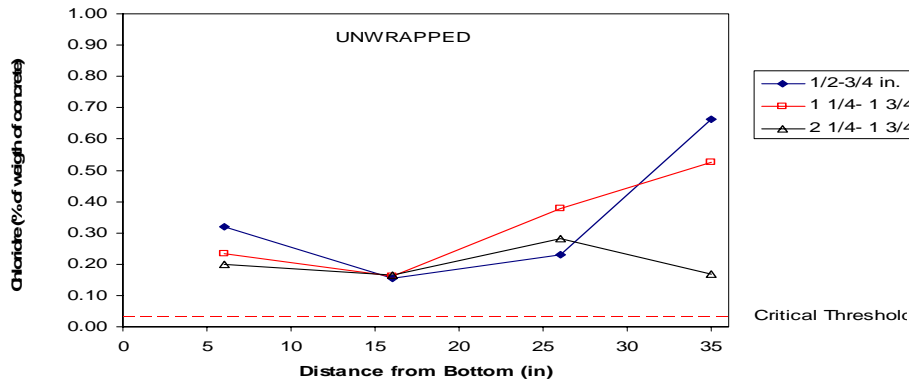


a) Corrosion activity

b) Half-cell potential profiles



c) Half-cell potential contours



d) Chloride content profiles

Figure 4.4 Data for Specimen CC11

4.2.3 CC17

Column CC17 was also a control specimen that contained no corrosion inhibitors. This cylinder was uncracked before placement in the monitoring tank and was repaired with latex modified concrete.

Wrap	None
Resin	None
Curing Agent	None
Surface	Dry
Crack Condition	Uncracked
Repair Material	LMC
Corrosion Inhibitor	None

Specimen CC17 was characterized by regions of rust staining and cracking across the entire surface. Although there were a few small stains near the bottom, the largest concentrations of rust staining occurred in the middle and upper sections. Two significant cracks were visible, one above rebar A over the entire height, and another above rebar D across the upper two-thirds.

The exposed rebar for this column showed wide-spread corrosion activity throughout the specimen (Fig. 4.5a). The most extensive corrosion appeared to be located in the lowest few inches and a large area approximately 12 inches from the bottom.

The half-cell potentials (Fig. 4.5b) recorded across this specimen indicate that severe corrosive activity was probably occurring over the entire height. The majority of data points are beyond the -500 mV threshold representing severe corrosion. The contour plot (Fig. 4.5c) reveals several areas where the highest readings appear to be concentrated 15 inches from the bottom and five inches from the top. These concentrations match visual observations.

The chloride content profile (Fig. 4.5d) follows the same upwards progression found in the preceding unwrapped specimens CC10 and CC11. All of the extracted samples fall well above the critical threshold needed for corrosion, matching up with the visual and half-cell readings.

CYLINDER CC17

Wrap	None
Resin	None
Curing Agent	None
Surface	Dry
Crack Condition	Uncracked
Repair Material	LMC
Corrosion Inhibitor	None

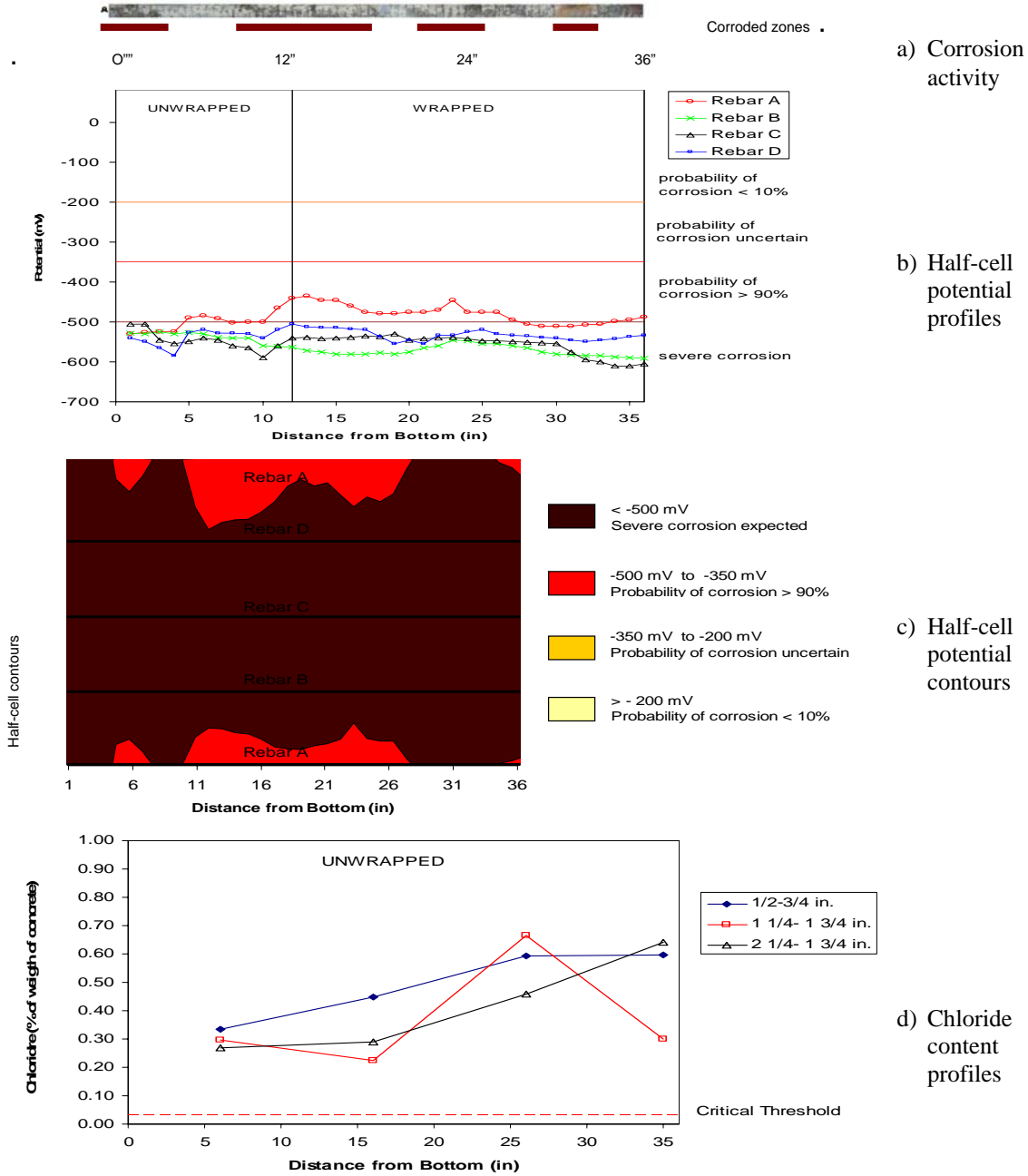


Figure 4.5 Data for Specimen CC17

4.2.4 CNC11

Column CNC11 features an extensive patched area around the midsection and a large area of latex-modified concrete (LMC) across most of the bottom. Additionally, this specimen features a concrete mix without added chlorides.

Wrap	None
Resin	None
Curing Agent	None
Surface	Dry
Crack Condition	Uncracked
Repair Material	LMC/Patch
Corrosion Inhibitor	None

Visual inspections indicated a few areas of rust staining near the midsection and lower areas. A large crack was noted near the repair materials between rebars A and D.

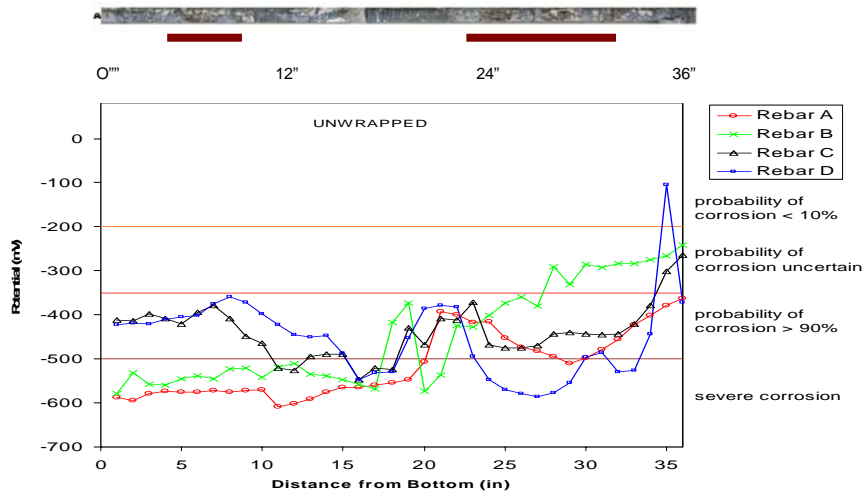
The exposed reinforcing steel in CNC11 showed the least amount corrosion activity of the unwrapped specimens (Fig. 4.6a). A small area of corrosion was noted approximately six inches from the bottom. Additionally, A wider area of corrosion could be found ranging five to twelve inches from the top.

The half-cell potentials obtained are presented in Figure 4.6b. The areas where the readings fluctuated are in the region that was patched with a repair material. The thick layers made it difficult to acquire data. However, despite the irregularities the trends on this graph and the contour plot in Figure 4.6c indicate that the corrosion activity is mostly confined to the lower areas, and drops off considerably near the top of the column.

This reduction in corrosion activity is further confirmed by the trends indicated in chloride content profile (Fig. 4.6d). Although the chloride levels at the top of the column are above the critical threshold, they are lower than in the previous specimens.

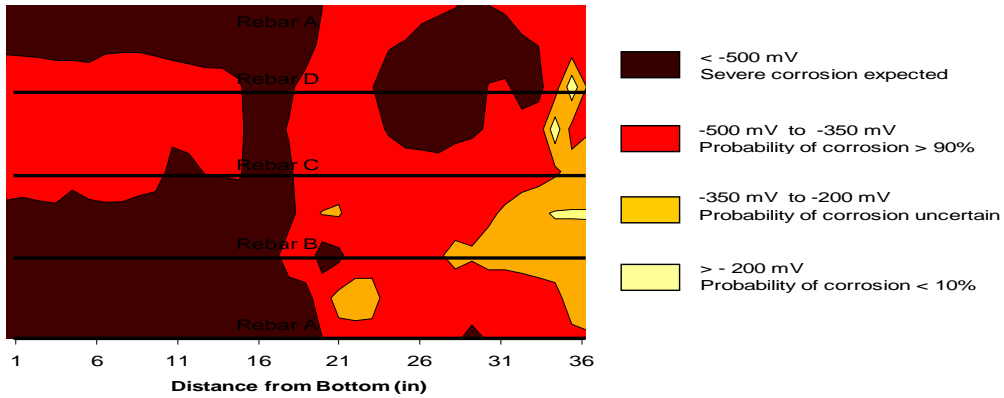
CYLINDER CNC11

Wrap	None
Resin	None
Curing Agent	None
Surface	Dry
Crack Condition	Uncracked
Repair Material	LMC/Patch
Corrosion Inhibitor	None

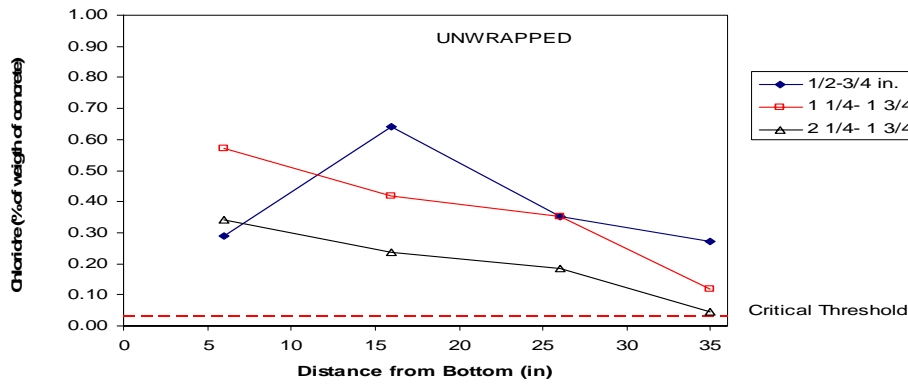


a) Corrosion activity

b) Half-cell potential profiles



c) Half-cell potential contours



d) Chloride content profiles

Figure 4.6 Data for Specimen CNC11

4.2.5 CNC20

Column CNC20 is the primary control specimen.

Wrap	None
Resin	None
Curing Agent	None
Surface	Dry
Crack Condition	Uncracked
Repair Material	None
Corrosion Inhibitor	None

Visual inspection indicated substantial activity along the entire height. There were several instances of staining and cracking, notably two large cracks that ran three inches from the top to nine inches from the bottom and seven inches from the top to four inches from the bottom above rebars C and D, respectively. The extracted reinforcing steel for this specimen exhibited extensive corrosive activity across most of the specimen. The only portion free from corrosion was the uppermost four inches (Fig. 4.7a).

The half-cell profiles for CNC20 indicated a strong probability of corrosion activity over the entire specimen (Fig. 4.7b). Almost every data point on both the linear rebar profile and the potential contours plotted in Figure 4.7c were beyond the -500 mV threshold for severe corrosion.

The chloride content data presented in Figure 4.7d is similar to that found in the other unwrapped specimens. An explanation of this phenomenon is discussed in detail in Chapter 5.

CYLINDER CNC20

Wrap	None
Resin	None
Curing Agent	None
Surface	Dry
Crack Condition	Uncracked
Repair Material	None
Corrosion Inhibitor	None

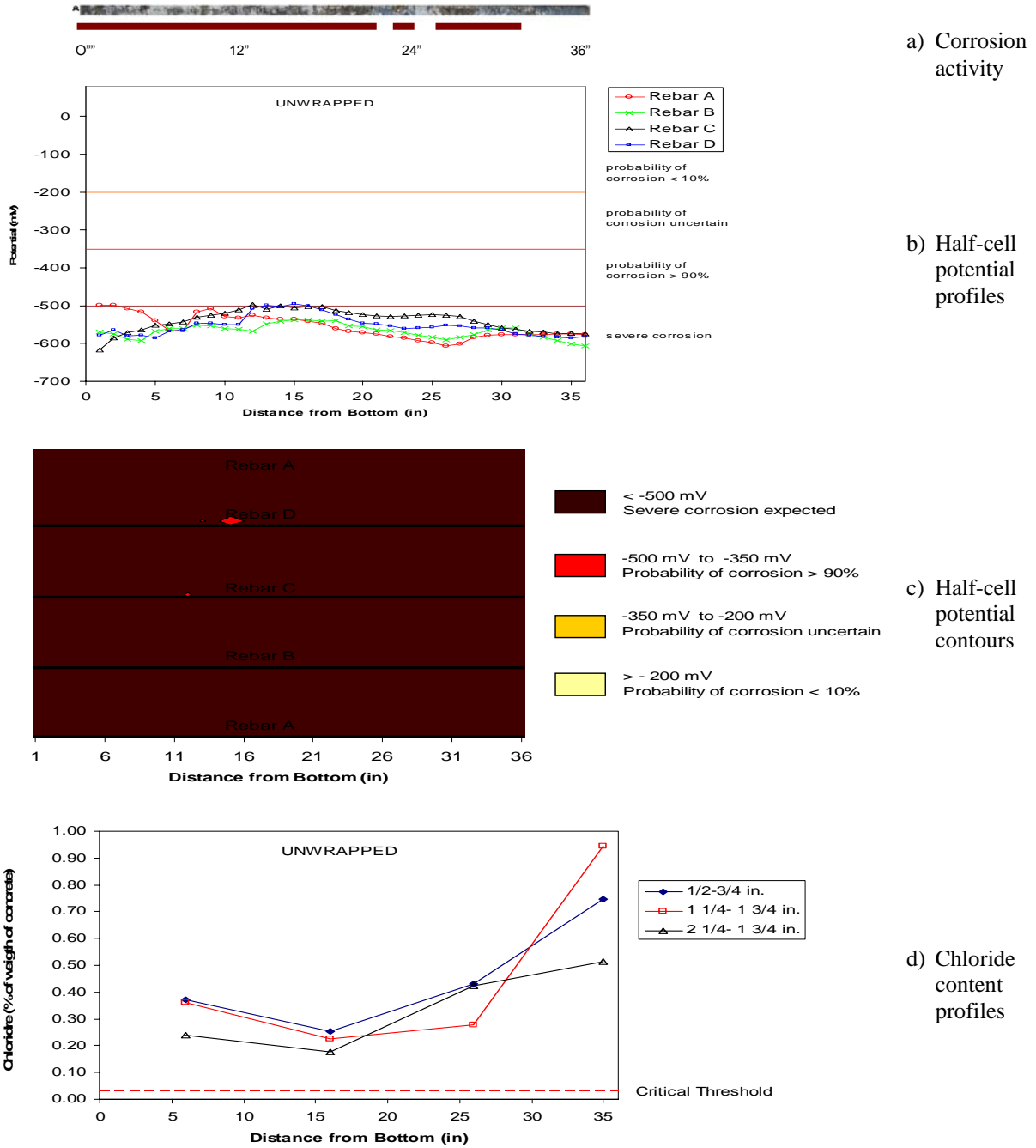


Figure 4.7 Data for Specimen CNC20

4.3 Wrapped Column Specimens

4.3.1 CC15

Column CC15 had a generic FRP wrap over the top 24” of the column and contained an inhibitor and an admixture.

Wrap	Generic 24-in.
Resin	862
Curing Agent	3090
Surface	Dry
Crack Condition	Cracked
Repair Material	None
Corrosion Inhibitor	Sika

After removal of the wrap, the exterior surface was characterized by a few small stains and interconnected cracks. The most significant feature indicating the presence of corrosion was a large diagonal crack located six inches from the top surface near rebar D that progressed to twelve inches from the bottom over rebar C. The exposed reinforcement exhibited two discrete regions of corrosion activity (Fig. 4.8a). One region of corrosion was located at bottom, and the other was located at the top.

The half-cell potential profiles for this specimen indicate the likelihood of corrosion at the lower and upper portions of the rebar (Fig. 4.8b). At the bottom of the specimen where the concrete was exposed to the salt-water environment, the potentials were at the -500 mV threshold. Almost directly at the 12-in. mark where the lower level of the FRP wrap began and extended upwards, the potential decreases dramatically. However, five inches from the top the potential increases rapidly and extends into the severe threshold. The contour plot clearly identifies the two regions where corrosion is observed on the exposed steel (Fig. 4.8c).

The chloride content profile for this specimen clearly demonstrates the ability of the FRP wrap to act as a barrier to chlorides (Fig. 4.8d). The exposed portion is marked by increased chloride concentrations. However, the concrete directly beneath the FRP wrap contains drastically reduced concentrations. Then, at the highest portion of the specimen the chloride content increases, which corresponds with the previously mentioned evidence of corrosion at the top of the column.

CYLINDER CC15

Wrap	Generic 24-in.
Resin	862
Curing Agent	3090
Surface	Dry
Crack Condition	Cracked
Repair Material	None
Corrosion Inhibitor	Sika

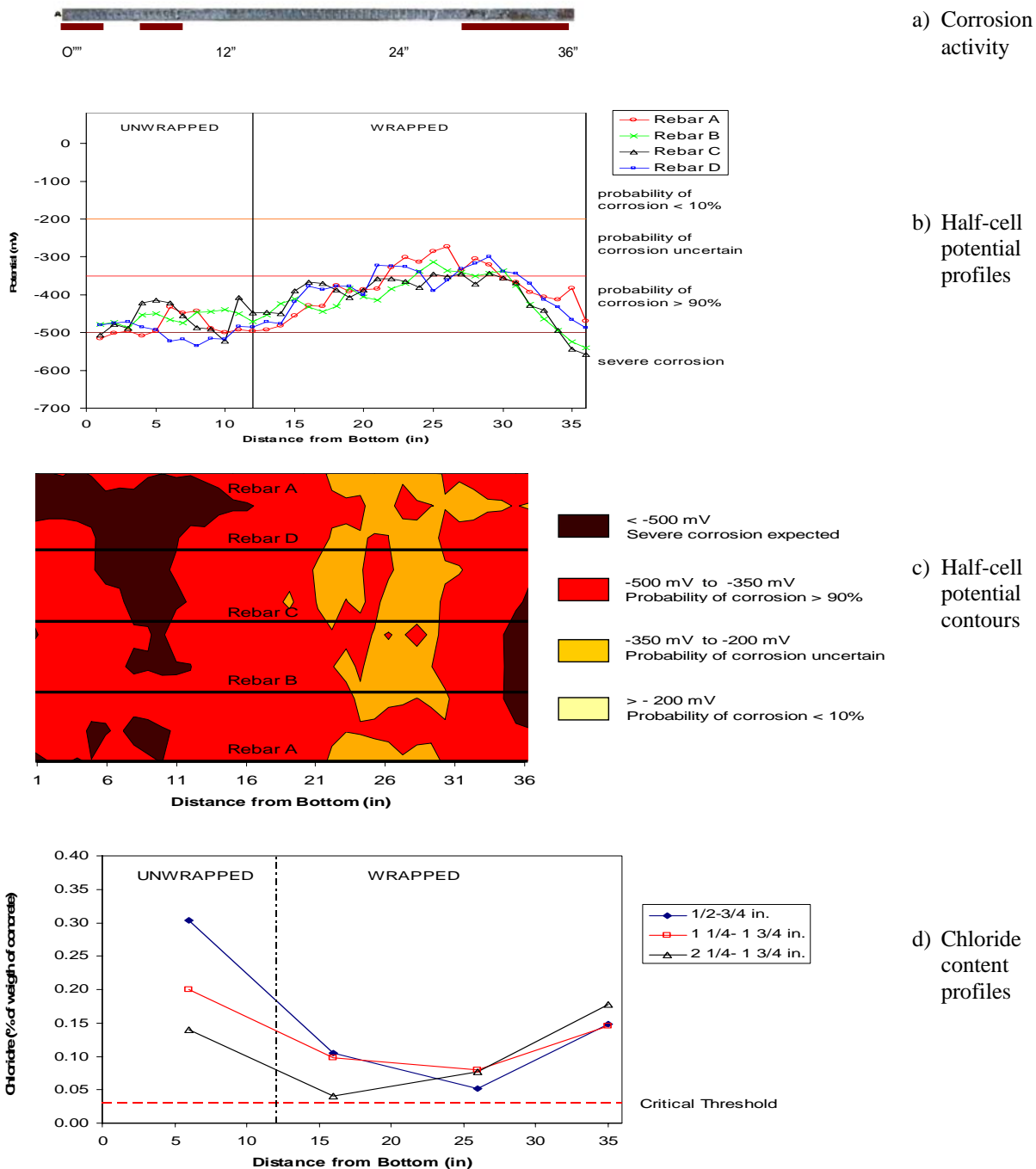


Figure 4.8 Data for Specimen CC15

4.3.2 CNC6

Specimen CNC6 had a generic wrap over the top 24 in. and contained a curing agent.

Wrap	Generic 24-in.
Resin	Vinyl
Curing Agent	411
Surface	Wet
Crack Condition	Cracked
Repair Material	Patch
Corrosion Inhibitor	None

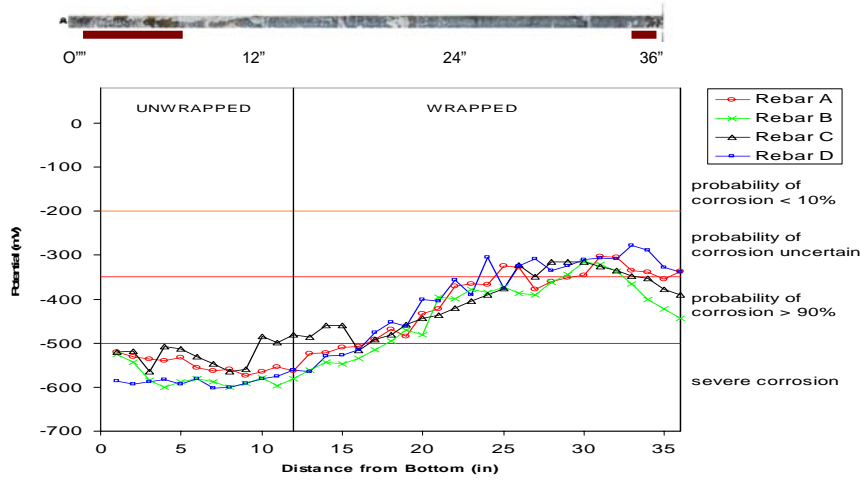
After the removal of the FRP wrap, there were few visual indications of corrosive activity. However, there were a few small areas of rust staining near the bottom of this specimen. The corrosion on the extracted rebar was limited to a length of about six inches from the bottom, and another two inches from the top. Most of the surface of the rebar between these two areas is free of corrosion (Fig. 4.9a).

The half-cell potentials for this specimen indicate the FRP wrap plays an important factor in limiting the corrosion activity throughout the covered portions of concrete. In Figure 4.9b, a rapid decrease in potential began at the 12-in. mark where the wrap ends. There is a small increase in potential near the top portion, which reflects the observed corrosion on the bar. The potential contour plot in Figure 4.9c shows the effect of the FRP wrap.

The chloride content profile (Fig. 9d) for specimen CNC6 mirrored the trends illustrated by the half-cell potential profiles. The exposed area of concrete at the bottom had a high chloride content and far beyond the critical threshold for corrosion to occur. However, samples of concrete from the center of the column behind the FRP wrap had low chloride concentrations, below the critical threshold.

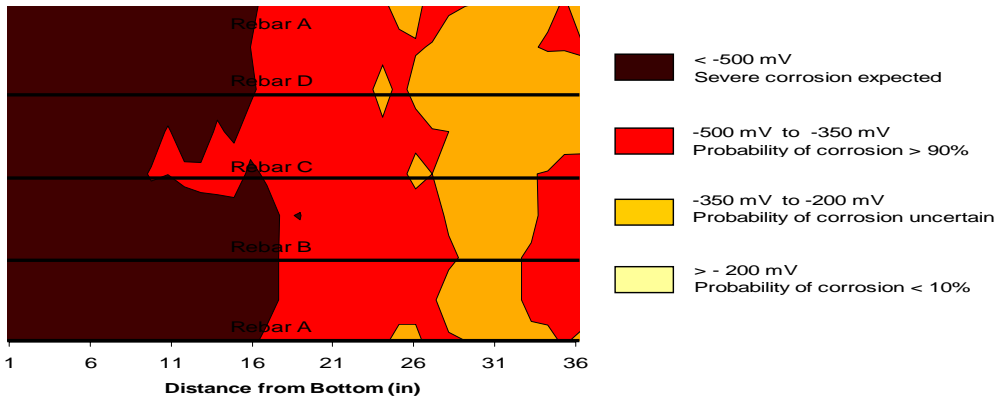
CYLINDER CNC6

Wrap	Generic 24-in.
Resin	Vinyl
Curing Agent	411
Surface	Wet
Crack Condition	Cracked
Repair Material	Patch
Corrosion Inhibitor	None

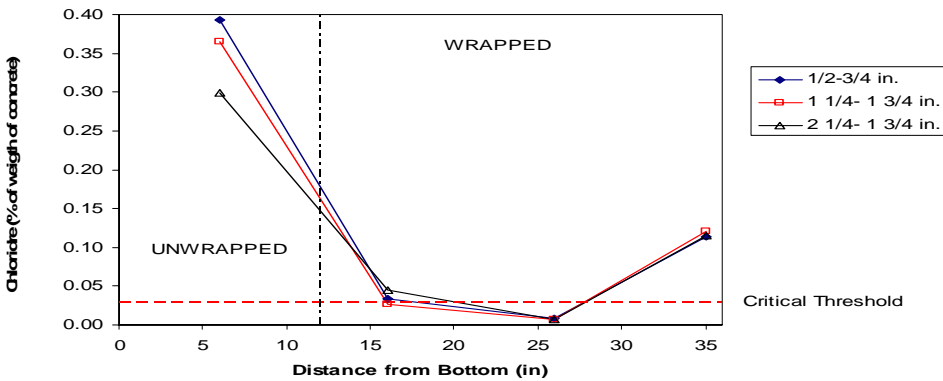


a) Corrosion activity

b) Half-cell potential profiles



c) Half-cell potential contours



d) Chloride content profiles

Figure 4.9 Data for Specimen CNC6

4.3.3 CNC16

Column CNC16 was wrapped with Delta system FRP material over the top 24 in.

Wrap	Delta 24-in.
Resin	Delta System
Curing Agent	Delta System
Surface	Dry
Crack Condition	Uncracked
Repair Material	LMC
Corrosion Inhibitor	None

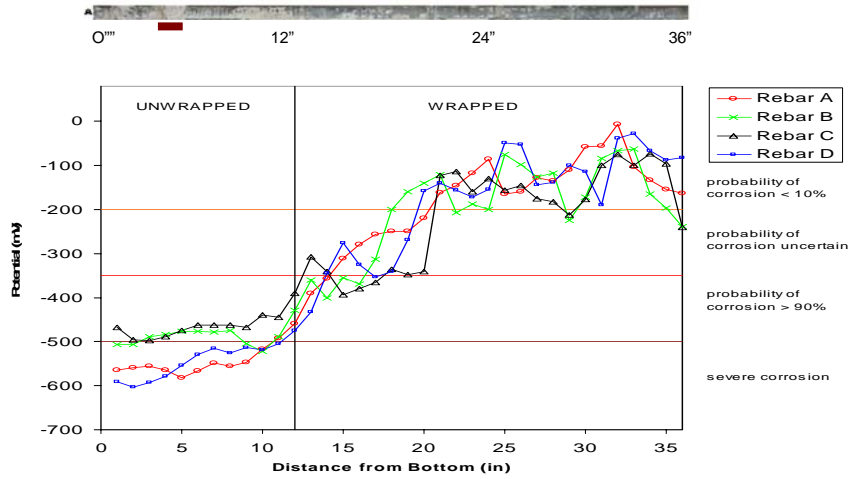
After the wrap was removed, the only visible indications of corrosion were a few instances of rust staining in areas where the concrete was routinely exposed to the salt-water environment. Inspection of the extracted reinforcement indicated that the only area of corrosion was a small region approximately five inches from the bottom. Overall, the rebar was almost entirely free of corrosion, as indicated by the photographs in Figure 4.10a.

The half-cell potential profiles for this specimen reveal a dramatic decrease in activity in the area beneath the FRP wrap (Fig. 4.10b). The only area where corrosion was visible is in the unwrapped portion and is reflected by their profiles which show virtually no potential activity within the wrapped region (Fig. 4.10c).

The chloride concentrations for this specimen (Fig. 4.10d) follow a trend similar to the other wrapped columns. However, the values here are dramatically lower. In fact, within the wrapped region the chloride content is practically zero, which explains the lack of corrosive activity across most of the rebar.

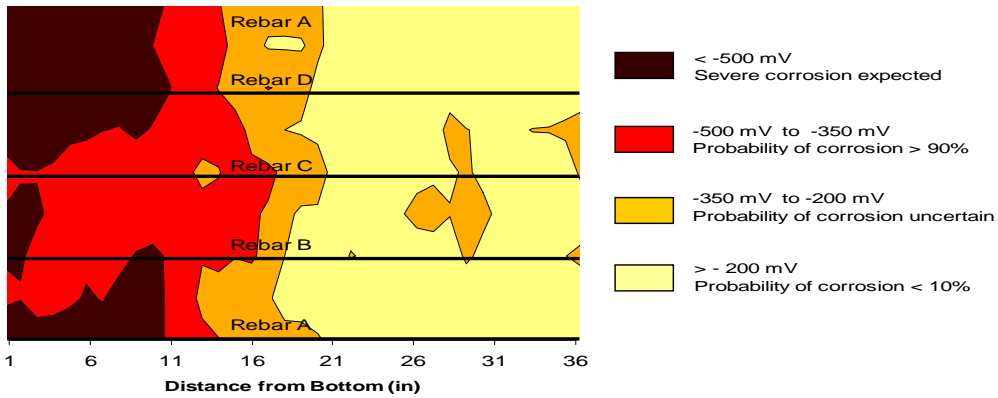
CYLINDER CNC16

Wrap	Delta 24-in.
Resin	Delta System
Curing Agent	Delta System
Surface	Dry
Crack Condition	Uncracked
Repair Material	LMC
Corrosion Inhibitor	None

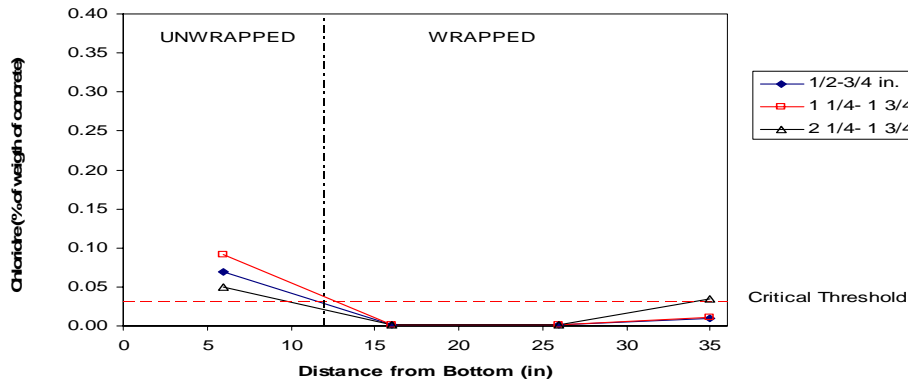


a) Corrosion activity

b) Half-cell potential profiles



c) Half-cell potential contours



d) Chloride content profiles

Figure 4.10 Data for Specimen CNC16

4.3.4 CNC17

This specimen had a Delta system wrap over the top 24 in.

Wrap	Delta 24-in.
Resin	Delta System
Curing Agent	Delta System
Surface	Dry
Crack Condition	Uncracked
Repair Material	EG
Corrosion Inhibitor	None

With the exception of a few incidents of rust staining at the bottom, most of the exterior of this column showed no serious corrosion. The only visible corrosive activity on the removed rebar was over the bottom four inches. The remaining surface of the reinforcing steel had no significant corrosion. A picture of this element is shown in Figure 4.11a.

The half-cell potential profiles for this specimen indicated a sharp decrease in the probability of corrosion beneath the wrapped portion of this column. Part of the concrete surface was patched with a non-reactive repair material, therefore, half-cell readings were not possible over much of the surface. Only two complete profiles were collected and are presented in Figure 4.11b. Similarly, the half-cell contour plot in Figure 4.11c reveals the dramatic decrease in activity within the wrapped region.

The chloride content profile (Fig. 4.11d) for CNC17 reveals a major factor for the lack of corrosion within the upper two-thirds of the column. The chloride concentration beneath the FRP wrap is practically zero for every sample collected within this region.

CYLINDER CNC17

Wrap	Delta 24-in.
Resin	Delta System
Curing Agent	Delta System
Surface	Dry
Crack Condition	Uncracked
Repair Material	EG
Corrosion Inhibitor	None

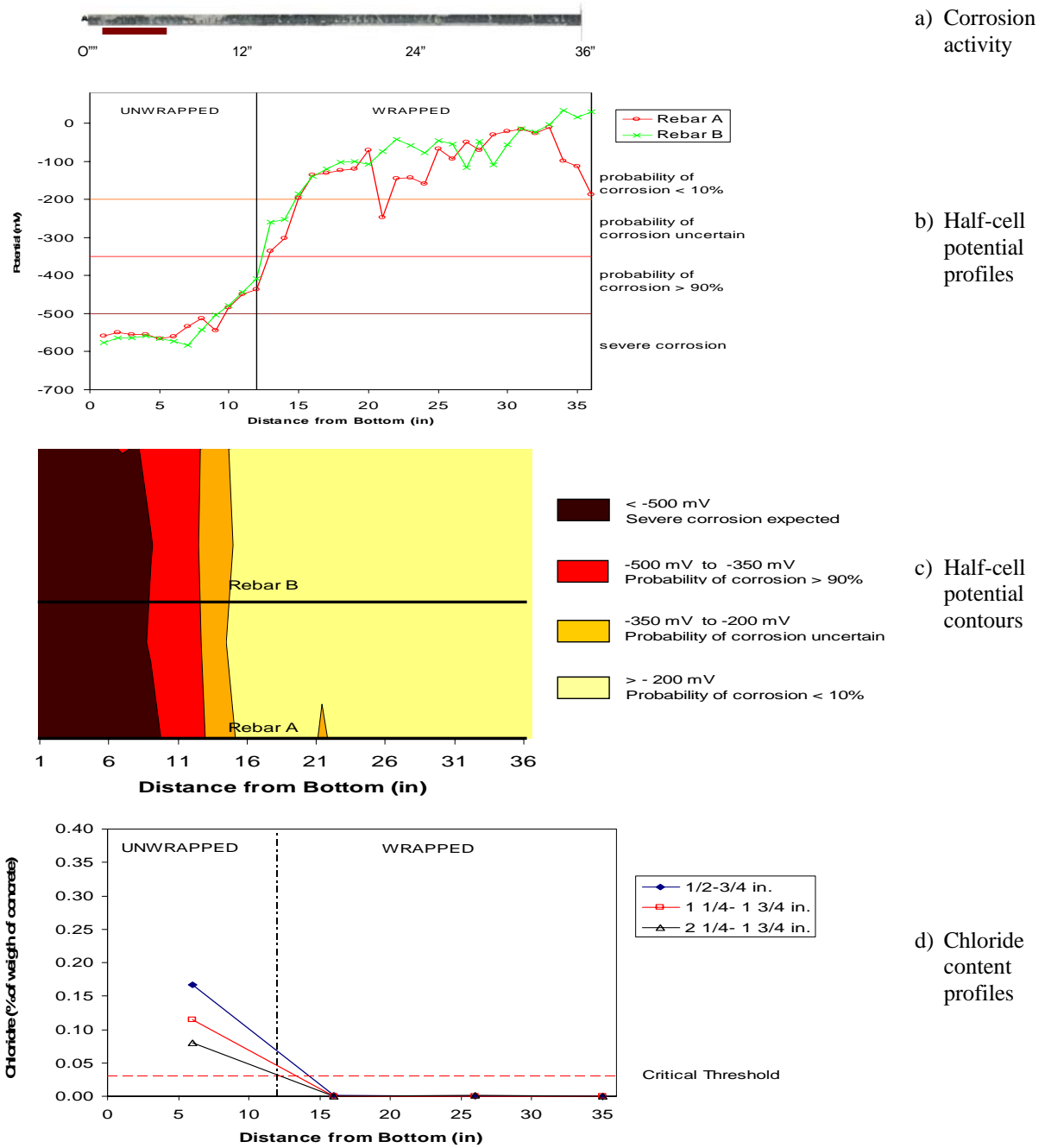


Figure 4.11 Data for Specimen CNC17

4.4 Unwrapped Beam Specimen

4.4.1 RNC2

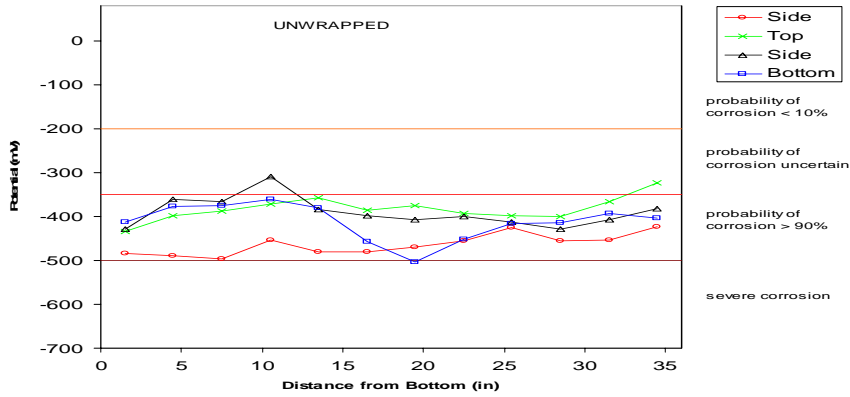
Beam RNC2 was a reference specimen with no corrosion protection. The concrete mix contained no corrosion inhibitor and no cast-in chlorides.

Wrap	None
Resin	None
Curing Agent	None
Surface	Dry
Crack Condition	Uncracked
Repair Material	None
Corrosion Inhibitor	None

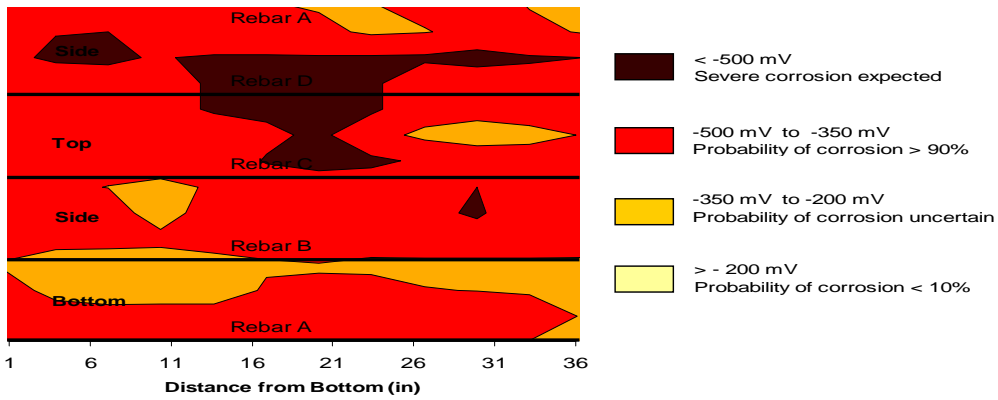
The beam specimens were slightly inclined so that the salt water would flow away (toward the bottom) from the end with exposed bars (top). Bars have not been removed from the specimens but chloride contents have been obtained. Nearly all potential readings (Fig. 4.12a) fall beyond the limit for 90% probability of corrosion. The half-cell contours indicate several areas where severe corrosion is expected (Fig 4.12b). The chloride content profile (Fig 4.12c) shows that chloride contents were above the threshold.

BEAM RNC2

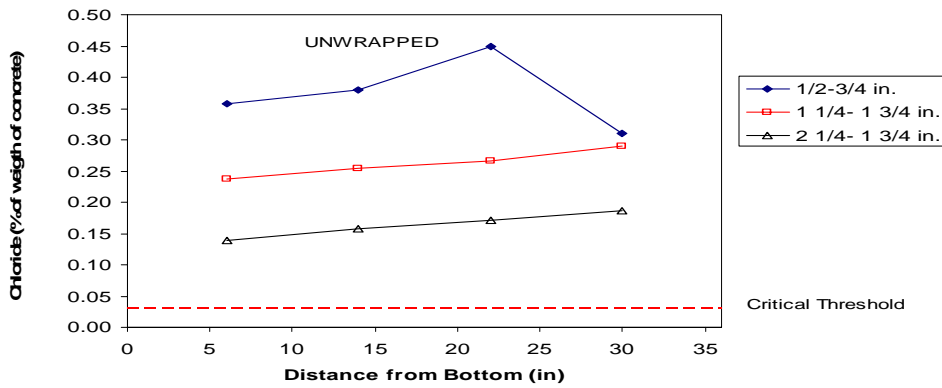
Wrap	None
Resin	None
Curing Agent	None
Surface	Dry
Crack Condition	Uncracked
Repair Material	None
Corrosion Inhibitor	None



a) Half-cell potential profiles



b) Half-cell potential contours



c) Average chloride content profiles

Figure 4.12 Data for Specimen RNC2

4.5 Wrapped Beam Specimens

4.5.1 RC3

This specimen was wrapped with a Delta system over the bottom 24 in. The concrete mix contained no corrosion inhibitor

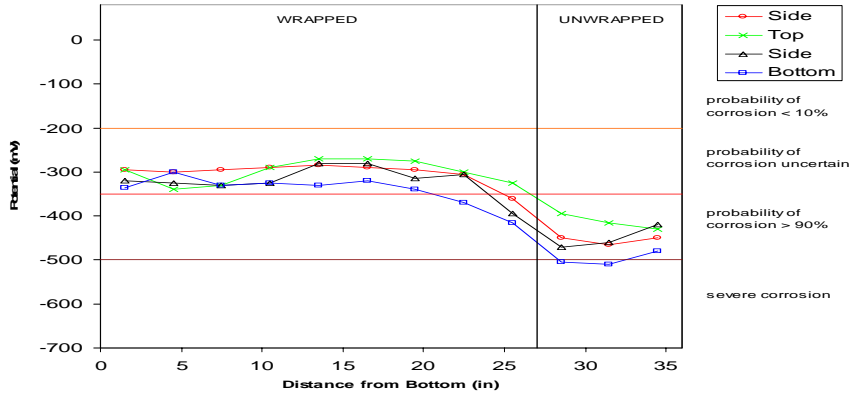
Wrap	Delta 24
Resin	Delta system
Curing Agent	Delta system
Surface	Dry
Crack Condition	Cracked
Repair Material	None
Corrosion Inhibitor	None

The half-cell profiles and contours (Figures 4.13a and b) show that most of the data points in the wrapped portion are at a level where the probability of corrosion is uncertain. In contrast, most data points in the unwrapped zone are at a level where the probability of corrosion is higher than 90%.

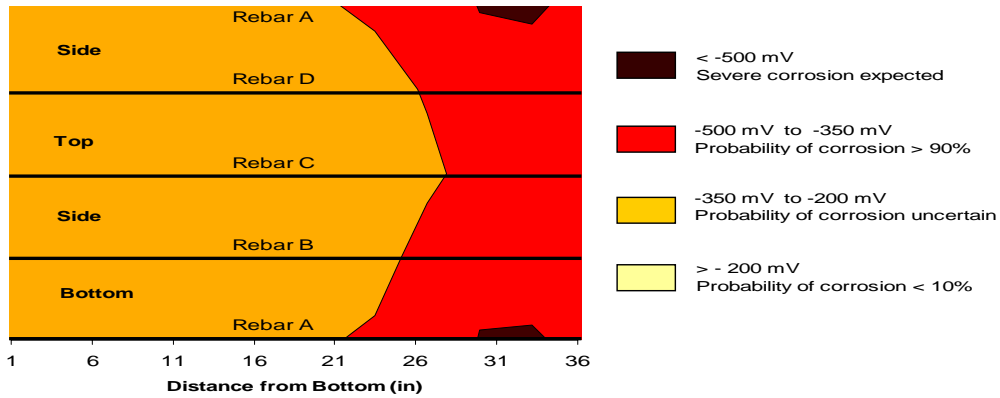
Chloride-content profiles (Fig 4.13c) indicate that the chloride levels are about the same in both zones and are higher than the 0.03 threshold. The chloride contents in RC3 were not as high as in specimen RNC2.

BEAM RC3

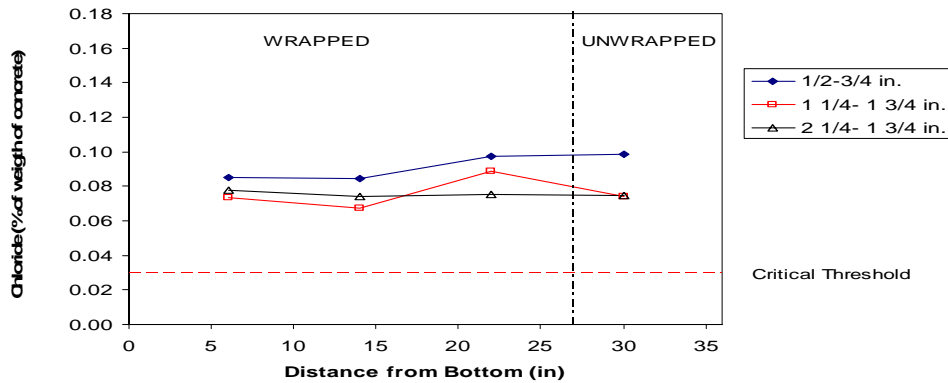
Wrap	Delta 24"
Resin	Delta system
Curing Agent	Delta system
Surface	Dry
Crack Condition	Cracked
Repair Material	None
Corrosion Inhibitor	None



a) Half-cell potential profiles



b) Half-cell potential contours



c) Average chloride content profiles

Figure 4.13 Data for Specimen RC3

4.5.2 RC5

This specimen was wrapped with Delta system materials over the bottom 27 in.

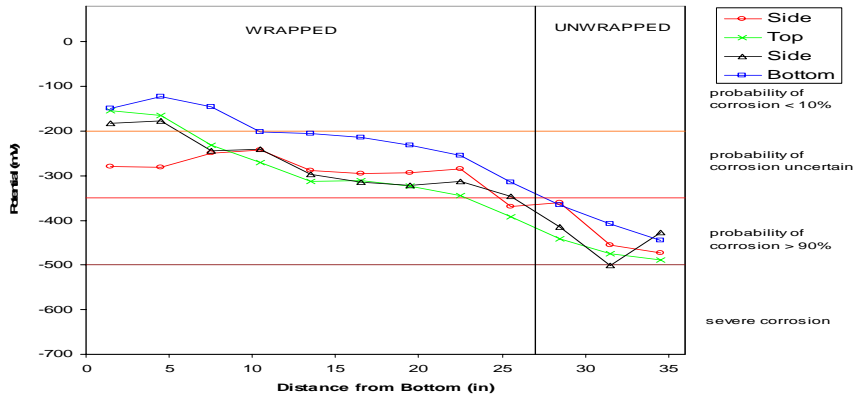
Wrap	Delta 27
Resin	Delta sytem
Curing Agent	Delta system
Surface	Dry
Crack Condition	Uncracked
Repair Material	LMC
Corrosion Inhibitor	None

In the half-cell profiles and contours (Figures 4.14a and b) most of the readings in the wrapped portion are at a level where the probability of corrosion is uncertain or less than 10%. In the unwrapped zone, most data points are in the zone with probability of corrosion higher than 90%.

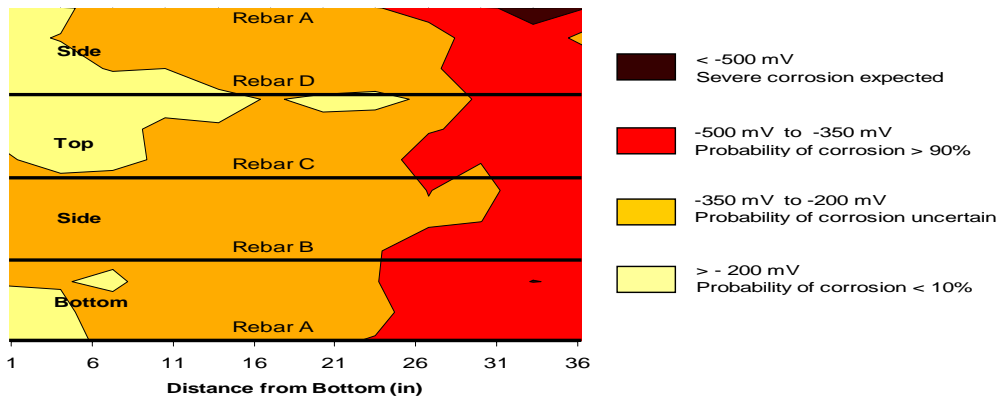
The chloride contents (Fig 4.14c) are significantly lower in the top and bottom surfaces of the wrapped zone. The chloride contents are slightly higher than the threshold in the wrapped zone and tend to increase toward the unwrapped end but are still considerably lower than the values in RNC2.

BEAM RC5

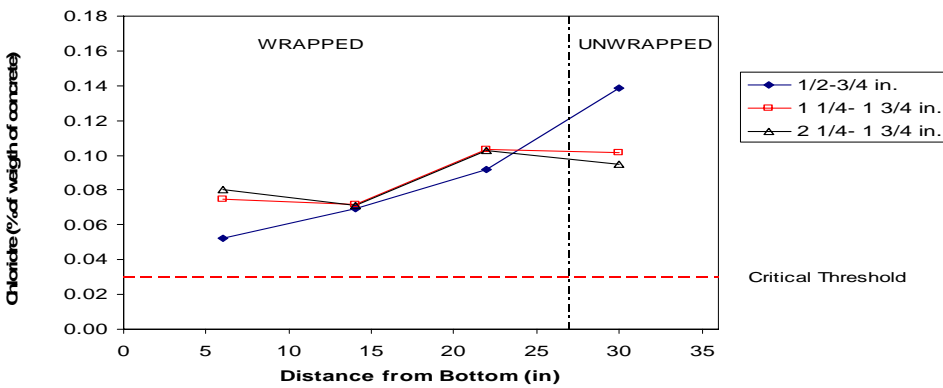
Wrap	Delta 27"
Resin	Delta system
Curing Agent	Delta system
Surface	Dry
Crack Condition	Uncracked
Repair Material	LMC
Corrosion Inhibitor	None



a) Half-cell potential profiles



b) Half-cell potential contours



c) Average chloride content profiles

Figure 4.14 Data for Specimen RC5

4.5.3 RNC1

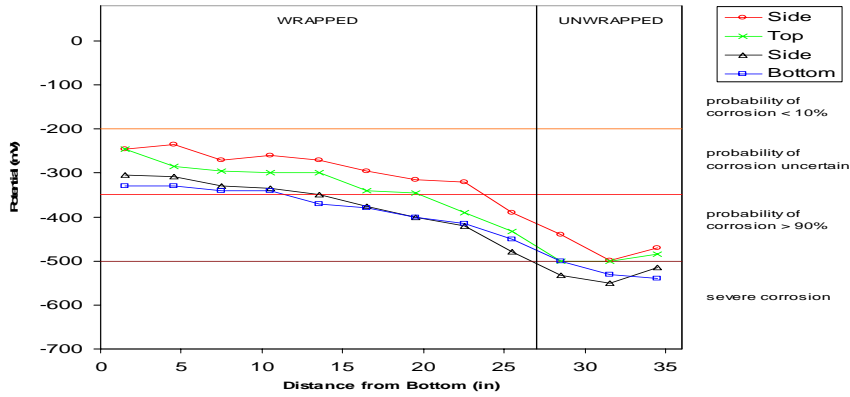
This specimen was wrapped with the Delta system over the bottom 24 in.

Wrap	Delta 24"
Resin	Delta system
Curing Agent	Delta system
Surface	Dry
Crack Condition	Uncracked
Repair Material	None
Corrosion Inhibitor	None

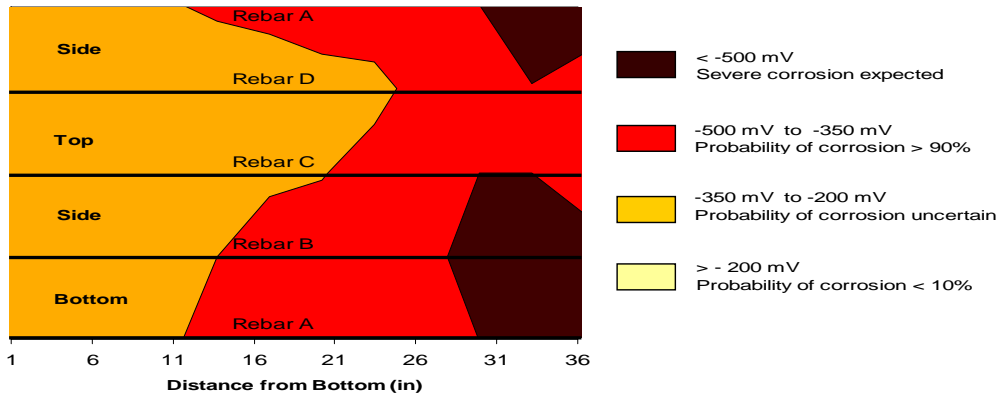
The half-cell profiles and contours (Figs. 4.15a and b) show trends similar to the other wrapped beams. Chloride content profiles (Fig. 4.15c) are low (generally less than 0.03) throughout.

BEAM RNC1

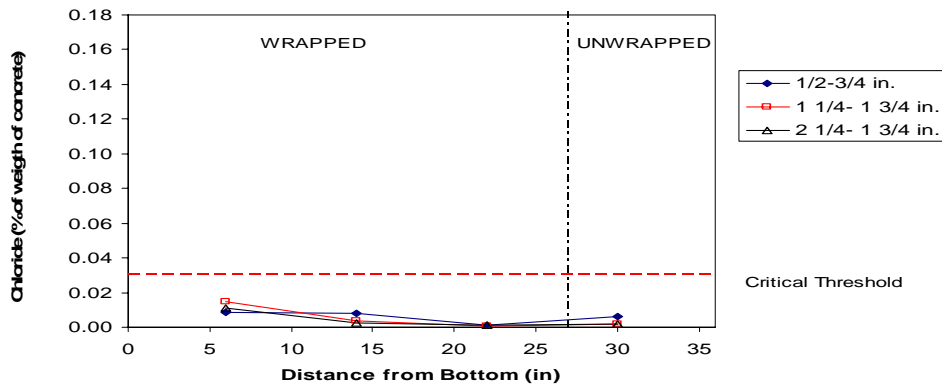
Wrap	Delta 24"
Resin	Delta system
Curing Agent	Delta system
Surface	Dry
Crack Condition	Uncracked
Repair Material	None
Corrosion Inhibitor	None



a) Half-cell potential profiles



b) Half-cell potential contours



c) Average chloride content profiles

Figure 4.15 Data for Specimen RNC1

5. Discussion of Results

5.1 Introduction

In the preceding chapter, a large amount of data on the corrosion behavior of a number of reinforced concrete specimens was presented. Although trends and observations were provided for each specimen, no correlations between specimens were not provided. The overall effectiveness of the FRP wraps and other admixtures for improving the durability of reinforced concrete in a corrosive environment was not evaluated.

5.2 Effectiveness of FRP Wrap

A main objective of the project was to evaluate the FRP wraps with respect to reducing corrosion of the imbedded reinforcing steel. Some have contended that the impervious barrier of the wrapping material prevents the escape of chlorides or other containments from the concrete. Thus, what is intended to prevent the ingress of materials producing corrosion might trap the chlorides already present in the mixture and have little influence on the corrosive process. On the other hand, the FRP wrap may be an effective barrier that prevents chloride-induced corrosion from occurring. To determine the effectiveness of the FRP wrap, half-cell potential profiles and chloride content profiles for different specimens are compared.

5.2.1 Comparison of Half-Cell Potentials

Figure 5.1 shows the average half-cell profiles recorded for the longitudinal bars in the column specimens. The unwrapped columns are plotted in Figure 5.1a, and the wrapped columns are shown in Figure 5.1b.

The columns exhibit almost identical behavior within the bottom twelve inches where no wrapping was applied. Each of the nine specimens has an average potential that fluctuates around the -500 mV threshold. However, above 12-in, potential readings in the wrapped specimens are much lower, some well below the 95% probability of corrosion. The potential readings for unwrapped columns remain at the severe corrosion level along the entire column height.

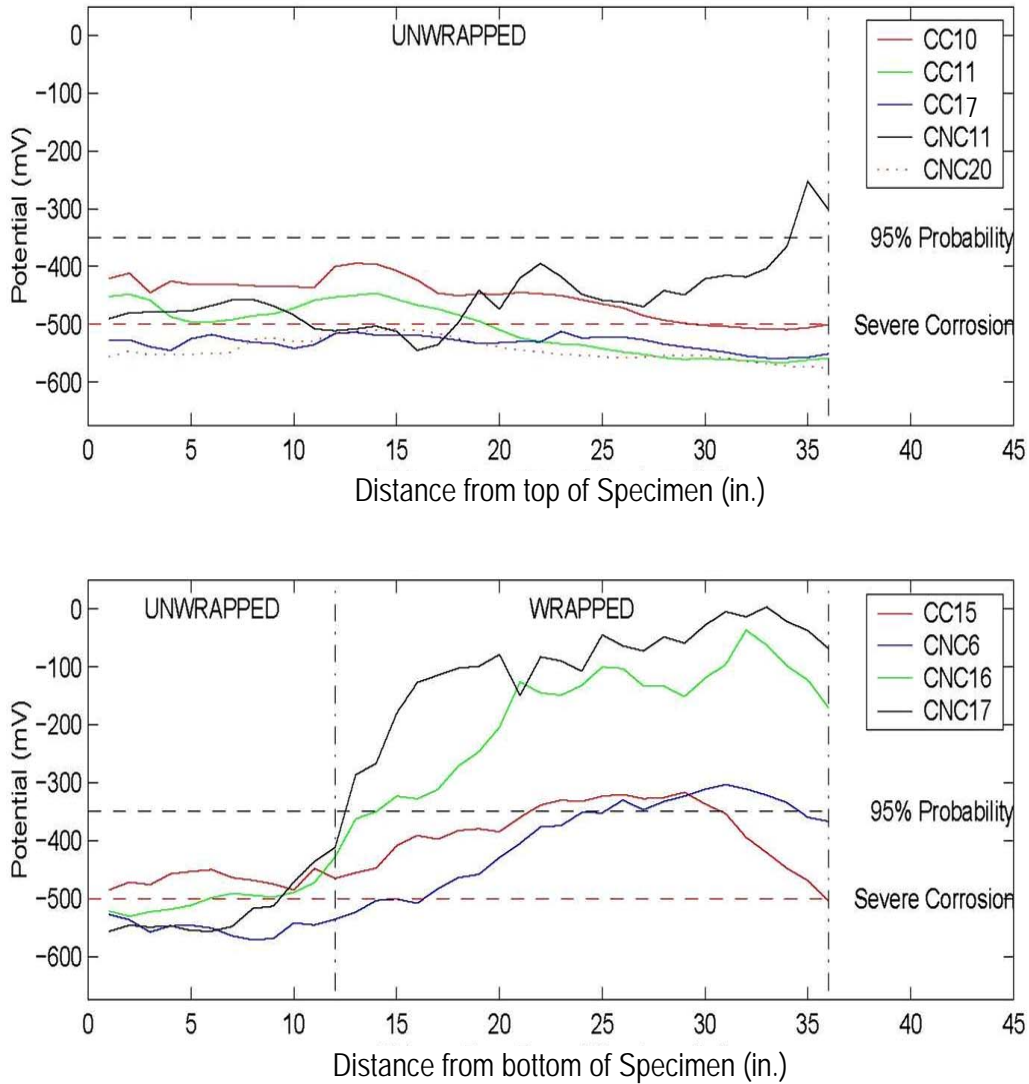


Figure 5.1 Average half-cell potential profiles for column specimens

Average half-cell profiles recorded above the four embedded rebars for the beam specimens are shown in Figure 5.2. The potential readings for the unwrapped beam, RNC2, are between -350 and -500 mV, along its entire length. Potentials along the wrapped sections are between -200 and -350 mV and increase at the wrapped ends to values similar to those of RNC2.

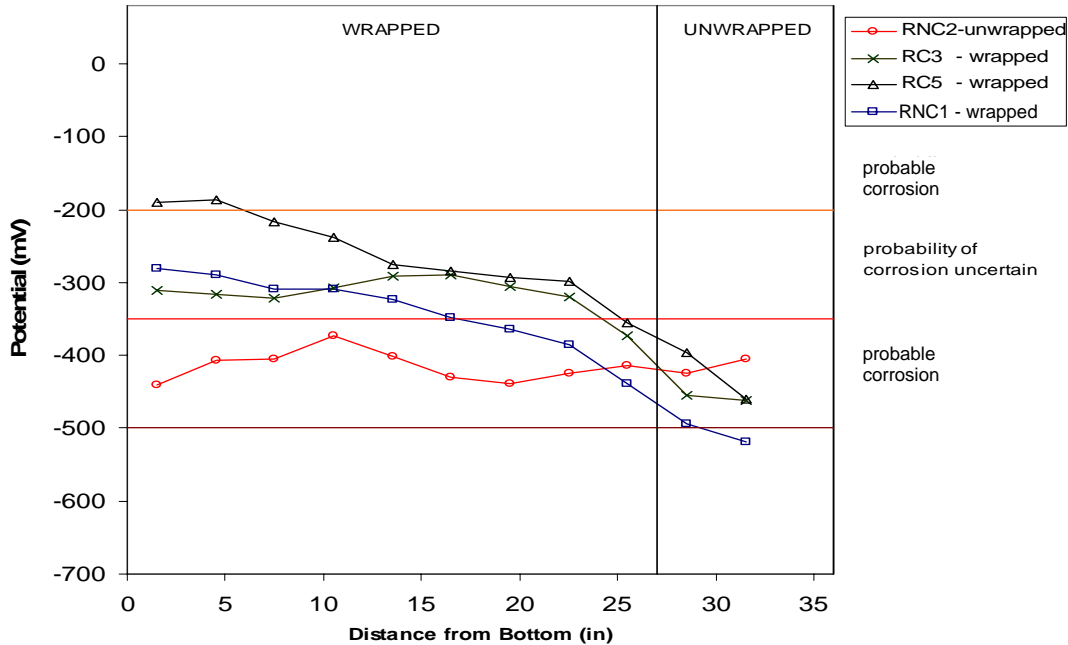


Figure 5.2 Average half-cell potential profiles for beam specimens

Comparisons of potentials provide strong indication that the addition of the FRP wrap reduced the likelihood of corrosion within the nine columns and four beams.

5.2.2 Chloride Contents

In Figure 5.3, the chloride content profiles exhibit the same trends as the half-cell potentials for wrapped and unwrapped columns.

For four of the five unwrapped columns, the chloride content increased from bottom to top of the columns. This trend was not expected because it would seem that higher concentrations should be found closer to the salt-water environment.

The wrapped columns showed a drastically different pattern. The concrete samples collected within the lower twelve inches for both groups range from 0.10% to 0.4%. However, samples collected from wrapped sections had low concentrations of chlorides near the 0.03% critical threshold.

The chloride contents (Fig. 5.4) for beams showed the same trends as those for the half-cell data. The chloride contents were significantly lower for the wrapped specimens

Clearly, the FRP wrapping limited the influx of chlorides to the upper portions of the columns. By comparing these chloride concentrations and the photographs of the extracted bars that had very little corrosion above the lower twelve inches, the effectiveness of FRP wrapping as a protection strategy becomes clearer.

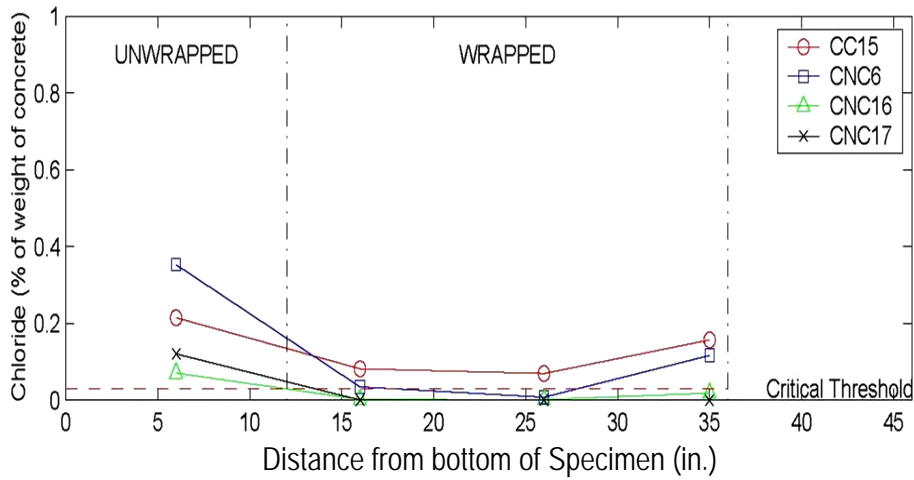
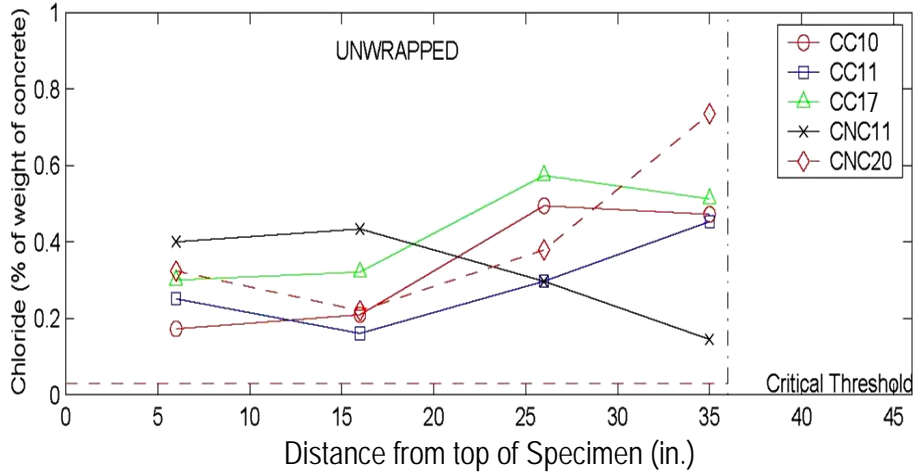


Figure 5.3 Average chloride content profiles for column specimens

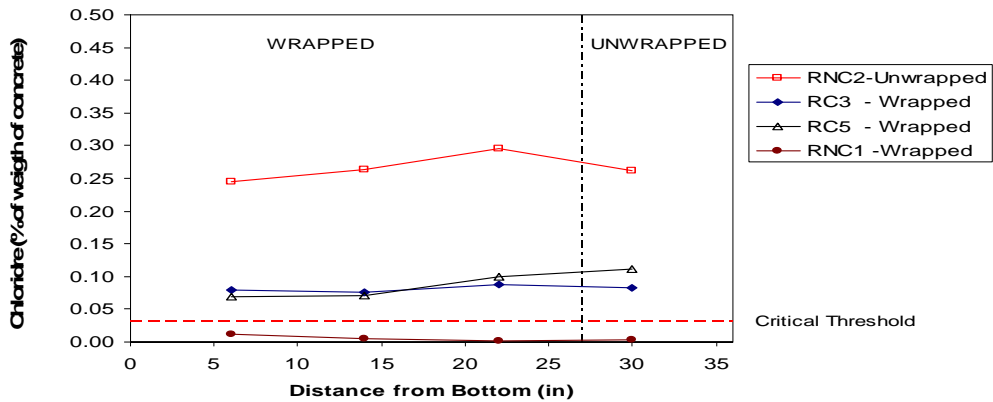


Figure 5.4 Average chloride contents for beam specimens

5.3 Effect of Other Variables

In addition to comparing the overall behavior of unwrapped and wrapped specimens, the data were also examined to determine the effect of the other parameters included in the group. The parameters are listed in Table 5.1 for the column specimens and the percentage of average half-cell readings that fall below the thresholds; -350 mV (>90% probability of corrosion) and -500 mV (severe corrosion likely). Only the column specimens were examined in this manner. There were too few beams to permit comparison.

Table 5.1 Statistical comparison presenting percentage of data points beyond given thresholds

Specimen	% below -350 mV	% below +-500 mV	Cast-in Chlorides	Wrap	Pre-cracked	Repair material	Corrosion Inhibitor
CC10	100	19	Yes	None	No	No	Ferrogard
CC11	100	53	Yes	None	No	No	None
CC15	75	3	Yes	Generic	Yes	No	Ferrogard
CC17	100	100	Yes	None	No	LMC	None
CNC6	75	44	No	Generic	Yes	Patch	None
CNC11	92	22	No	None	No	LMC	None
CNC16	39	17	No	Delta	No	LMC	None
CNC17	33	22	No	Delta	No	EG	None
CNC20	92	22	No	None	No	No	None

5.3.1 Cast-in Chlorides

Potential readings were lower for specimens that had no chlorides cast in the concrete. The presence of chlorides prior to wrapping reduced the effectiveness of the wrapping as measured by the percentage of readings below both threshold levels.

5.3.2 Unwrapped Specimens

For the five specimens that were not wrapped, the percent of readings below -350 mV was about the same for all, ranging from 92% to 100%. However, CC10, CNC11 and CNC20 had a low percentage of readings below -500 mV. CC10 had a corrosion inhibitor applied, and none were pre-cracked. Visual inspection of the rebar from CNC11 confirmed that there was less corrosion when compared with the other unwrapped columns.

5.3.3 Repair/Repair Materials

CC17, CNC6, CNC11, CNC16 and CNC17 were repaired. CC17 and CNC6 were pre-cracked. Latex-modified concrete repair material is less permeable than ordinary concrete. The lower permeability of the LMC might have prevented the migration of chlorides upwards through the column. However, the only specimen that showed a *decrease* in chloride content upwards through the column is CNC11. The other specimens all show an increase in chloride content.

5.3.4 Precracking

The highest percentage of readings below -500 mV was observed for CC11, CC17 and CNC6. CNC6 was pre-cracked, but had no cast-in-chlorides and was wrapped. The only difference between CC11 and CC17 was repair with LMC. Pre-cracking may lead to

higher half-cell potentials in the early stages of exposure but did not seem to be a consistent factor in the performance after a long period of exposure.

5.3.5 Corrosion Inhibitors

Two specimens (CC10 and CC15) were treated with Ferrogard corrosion inhibitor. Both had cast-in chlorides. Both exhibited low percentages of readings below -500 mV. CC15 had the lowest percentage (3%) of readings below -500 mV. The corrosion inhibitor appears to have improved the performance of those two specimens in this group.

6. Conclusions and Recommendations

6.1 Summary

The service life of many transportation structures is controlled by corrosion. The durability of reinforced concrete structures is a critical design issue, yet it is one of the least understood components of the design process for most engineers. Economic and reliable solutions are needed to extend the design life of structures in a corrosive environment.

One method that has been used for protecting concrete structures from corrosion is wrapping of structural elements with fiber reinforced plastic (FRP) composite materials. By placing an impermeable barrier around the surface of the concrete, the intent is to prevent corrosive materials such as chlorides from entering and initiating a chemical process that may eventually destroy embedded reinforcing steel and the surrounding concrete. There is little reliable data regarding the long-term effectiveness of FRP wraps for preventing corrosion in reinforced concrete structures.

The purpose of this program was to study the long-term behavior of beam and column laboratory specimens exposed to an aggressive chloride-rich environment. The project was designed to develop a better understanding of the long-term effects of FRP wrapping in preventing corrosion in reinforced concrete structures. Project 0-1774 involves both rectangular (beam) and cylindrical (column) specimens for which the effect of partially wrapped versus unwrapped elements was studied. Other parameters of interest in design and construction included: cast-in chlorides to represent specimens already exposed to a corrosive environment prior to wrapping, cracked versus uncracked elements, addition of corrosion inhibitors, and repair of damage to concrete due to corrosion or to construction traffic prior to wrapping.

6.2 Conclusions

From the nine column and four beam specimens that were extensively studied after removal from an environment that produced accelerated corrosion, the major findings to date are as follows:

1. The FRP wrap appeared to play a significant role in providing a barrier to the migration of chlorides throughout the reinforced concrete element. Half-cell potential readings were higher (indicating a reduced probability of corrosion) for the wrapped portions of the specimens. The chloride concentrations within the unwrapped portion of the test specimen were equivalent to those obtained in the totally unwrapped specimens. The condition of extracted bars corroborated the potential readings and chloride contents, that is, more corrosive damage was evident where potentials were lower and chloride levels were high. One unexpected finding was the increase in chloride content at higher locations in the unwrapped specimens.

2. Corrosion damage was more severe in specimens with cast-in chlorides.

3. Cracked specimens appeared to reach severe corrosion levels more rapidly than uncracked specimens, however the number of specimens studied was very small.

4. The two column specimens with chloride inhibitors had lower half-cell potential readings than those without (seven specimens).

It is interesting to note that while the chronological record provides some indication of trends, the fact that half-cell readings are taken at only a few locations (one reading in wrapped zone), it is very difficult to formulate conclusions based on the chronological record. The extensive analysis described in this report would appear to be the most desirable way to evaluate the influence of the parameters included in the study.

6.3 Recommendations

Some of the exposed reinforcing steel corroded due to the extremely aggressive environment of the exposure tank. This exterior corrosion could spread to areas beneath the surface, and subsequently affect the outcome of the experiment. It is recommended that in future projects exposed reinforcing steel be removed or reduced in order to limit the introduction of exterior corrosion. The bars could have been sawed off at the surface and there would still have been enough surface contact to conduct half-cell profile readings.

Another recommendation is that a clearer system of systematically studying the various design parameters be considered. In this project, a large number of variables were included and complicated the process of identifying which factors directly contribute to reducing corrosion. In future studies, the total number of parameters should be reduced or a process developed so that the effects of a given parameter can be clearly established.

References

- American Society of Civil Engineers. "Report Card for America's Infrastructure: Bridges," American Society of Civil Engineers. 2001.
- ASTM. "Standard Test Method for Half-Cell Potential of Uncoated Reinforcing Steel in Concrete," Annual Book of ASTM Standards, Designation: C876-87, ASTM: West Conshohocken, PA, pp. 428-432. 1989.
- Berver, E.W., Jirsa, J. O., Fowler, D.W., Wheat, H.G., and Moon, T., "Effects of Wrapping Chloride Contaminated Concrete with Fiber Reinforced Plastics," Center for Transportation Research Report 0-1774-2, October 2001.
- Berver, Emily Wason. "Effects of Wrapping Chloride Contaminated Concrete with Fiber Reinforced Plastics," M.S. Thesis, Civil Engineering Department, University of Texas at Austin. 2001.
- Callister, Jr., William D. Materials Science and Engineering: An Introduction. NY: John Wiley & Sons, Inc., 2000.
- Carino, Nicholas J. "Nondestructive Techniques to investigate corrosion status in concrete structures," Journal of Performance of Constructed Facilities. 13:3, 1999. pp 96 – 106.
- Chess, P.M. Cathodic Protection of Steel in Concrete. NY: E & FN Spon, 1998.
- Fuentes, Laura Alexandra. "Implementation of Composite Wrapping Systems on Reinforced Concrete Structures Exposed to a Corrosive Laboratory Environment," Thesis, Civil Engineering Department, University of Texas at Austin. 1999.
- Mattsson, Einar. Basic Corrosion Technology for Scientists and Engineers. NY: Ellis Horwood Limited, 1989.
- Roberge, Pierre R. Handbook of Corrosion Engineering. NY: McGraw-Hill, 1999.
- Slater, John E. Corrosion of Metals in Association with Concrete. Ann Arbor, MI: ASTM, 1983
- Van Deveer, J.R. *Journal of the American Concrete Institute*. Vol. 12, 1975.
- Verhulst, S. M., Fuentes, L.A., Jirsa, J. O., Fowler, D.W., Wheat, H.G., and Moon, T., "Evaluation and Performance Monitoring of Corrosion Protection Provided by Fiber-Reinforced Composite Wrapping," Center for Transportation Report 0-1774-1, January 2001.
- Yunovich, Mark and Neil G. Thompson. "Corrosion of Highway Bridges: Economic Impact and Control Methodologies." *Concrete International*. January 2003. pp 52 – 57.

APPENDIX A: Test Specimen Characteristics, Status and Data

Table A-1 CHARACTERISTICS AND STATUS OF SPECIMENS

Specimen (a)	Status (b)	Wrap	Resin	Curing Agent	Surface at	Crack Condition	Repair Material	Corrosion Inhibitor
CC1	O	delta-24"	Tyfo S		dry	cracked	none	ferrogard
CC2	O	gen/del-30"	Tyfo S		wet	uncracked	LMC	none
CC3	R	delta-24"	Tyfo S		dry	uncracked	EG	none
CC4	O	delta-24"	Tyfo S		dry	uncracked	LMC	none
CC5	R	generic-36"	862	3234	dry	cracked	patch	none
CC6	R	generic-36"	vinyl ester		dry	cracked	patch	ferrogard
CC7	R	delta-24"	Tyfo S		dry	cracked	none	none
CC8	O	delta-36"	Tyfo S		dry	cracked	LMC	none
CC9	O	delta-24"	Tyfo S		dry	uncracked	none	none
CC10	R	none	none		dry	uncracked	none	ferrogard
CC11	R	none	none		dry	uncracked	none	none
CC12	O	generic-30"	862	3234	wet	cracked	none	none
CC14	O	generic-24"	862	3234	dry	uncracked	LMC	ferrogard
CC15	R	generic-24"	862	3090	dry	cracked	none	ferrogard
CC16	O	none	none		dry	uncracked	EG	none
CC17	R	none	none		dry	uncracked	LMC	none
CC18	R	none	none		dry	cracked	none	none
CC19	O	generic-24"	vinyl ester		dry	uncracked	LMC	none
CC20	O	generic-24"	vinyl ester	411	dry	uncracked	none	ferrogard
CC21	O	none	none		dry	cracked	none	ferrogard
CNC1	O	generic-27"	862	3234	wet	cracked	patch	none
CNC2	O	generic-36"	862	3234	dry	cracked	none	none
CNC3	O	generic-24"	862	3234	dry	uncracked	none	ferrogard
CNC4	O	delta-24"	Tyfo S		dry	uncracked	none	none
CNC6	R	generic-24"	vinyl ester		wet	cracked	patch	none
CNC7	O	none	none		dry	uncracked	none	ferrogard
CNC8	R	none	none		dry	cracked	none	ferrogard
CNC9	O	generic-24"	vinyl ester		dry	uncracked	LMC, patch	none
CNC10	R	delta-24"	Tyfo S		dry	cracked	none	none
CNC11	R	none	none		dry	uncracked	LMC, Patch	none
CNC13	R	generic-24"	862	3234	dry	cracked	none	ferrogard
CNC14	R	generic-36"	862	3234	dry	cracked	none	ferrogard
CNC15	O	none	none		dry	cracked	none	none
CNC16	R	delta-24"	Tyfo S		dry	uncracked	LMC	none
CNC17	R	delta-24"	Tyfo S		dry	uncracked	EG	none
CNC18	O	generic-24"	862	3234	dry	uncracked	LMC	ferrogard
CNC19	R	generic-24"	862	3234	dry	uncracked	none	none
CNC20	R	none	none		dry	uncracked	none	none
RC1	O	generic-27"	862	3234	dry	uncracked	LMC	ferrogard
RC3	R	delta-24"	Tyfo S		dry	cracked	None	none
RC4	R	none	none		dry	cracked	none	none
RC5	R	delta-27"	Tyfo S		dry	uncracked	LMC	none
RC6	O	gen/del-33"	862	3090	dry	uncracked	LMC	none
RC7	R	generic-30"	862	3234	dry	cracked	none	none
RC8	O	none	none		dry	uncracked	LMC	none
RC9	O	gen/delta-24"	862	3090	dry	cracked	none	ferrogard
RNC1	R	delta-24"	Tyfo S		dry	uncracked	none	none
RNC2	R	none	none		dry	uncracked	none	none
RNC4	O	generic-36"	vinyl ester		dry	uncracked	LMC	none
RNC5	O	delta-30"	Tyfo S		dry	cracked	none	none
RNC6	R	gen/delta-30"	862	3234	dry	cracked	LMC	none
RNC7	R	none	none		dry	cracked	none	none
RNC8	O	generic-24"	862	3234	dry	cracked	none	none

NOTES

- First letter of specimen name corresponds to cylinders [C] or beams [R]. If second letter is "N" there are no built in chlorides. Italicized rows indicate specimens autopsied and reported herein.
- Highlighted specimens are those that have been removed (R) from the tank and have been autopsied Ongoing tests (O).

Table A-2 CHRONOLOGICAL RECORD OF HALF-CELL READINGS OF SPECIMENS

Specimen (a)	Half-Cell Readings in Tank (mV)									
	4/18/2000 (b)	10/15/2000	2/5/2001	2/15/2002	3/5/2002	1/10/2003	2/10/2003	12/4/2003	12/16/2003	4/27/2003
CC1		-298		-304	-250	-322	-319	-360	-313	-355
CC2		-211		-276	-247	-280	-271	-300	-41	-373
CC3		-183	-212							
CC4		-238		-271	-165	-206	-194	-265	-353	-317
CC5		-438	-460							
CC6		-437	-459							
CC7	-607									
CC8		-324		-323	-304	-472	-481	-285	-301	-391
CC9		-270		-301	-221	-314	-284	-300	-1	-334
CC10		-398		-485	-398	-485	-412			
CC11		-432		-536	-252	-549	-485			
CC12		-269		-335	-237	-262	-250	-350	-18	-244
CC14		-344		-307	-285	-274	-281	-390	-343	-512
CC15		-330		-393	-324	-427	-360			
CC16		-324		-526	-440	-510	-460	-550	-480	-556
CC17		-385		-489	-430	-578	-498			
CC18	-590									
CC19		-248		-289	-266	-300	-270	-550	-466	-578
CC20		-291		-357	-294	-352	-320	-370	-280	-404
CC21		-389		-536	-446	-508	-429	-530	-457	-528
CNC1		-326		-360	-325	-398	-374	-460	-422	-483
CNC2		-401		-407	-376	-416	-407	-460	-477	-503
CNC3		-274		-375	-258	-349	-309	-420	-411	-445
CNC4		-386		-345	-305	-325	-298	-420	-418	-451
CNC6		-356		-451	-380	-485	-455			
CNC7		-487		-523	-448	-506	-483	-610	-541	-581
CNC8	-410									
CNC9		-327		-307	-416	-439	-417	-480	-451	-486
CNC10		-319	-356							
CNC11		-422		-541	-492	-549	-510			
CNC13	-611									
CNC14	-535									
CNC15		-418		-393	-485	-575	-393	-525	-3	-524
CNC16		-267		-332	-292	-319	-314			
CNC17		-227		-297	-229	-272	-255			
CNC18		-216		-323	-263	-306	-297	-380	-404	-421
CNC19	-556									
CNC20		-409		-572	-512	-563	-487			
RC1		-266		-485	-394	-304	-170	-450	-390	-431
RC3		-359		-343	-257	-328	-317			
RC4	-609									
RC5		-250		-208	-170	-127	-135			
RC6		-135		-123	-110	-145	-220	-265	-904	-516
RC7	-411									
RC8		-377		-513	-408	-471	-260	-470	-313	-535
RC9		-297		-246	-201	-204	-151	-620	-222	-432
RNC1		-226		-165	-140	-222	-221			
RNC2		-434		-273	-350	-456	-416			
RNC4		-265		-267	-235	-173	-200	-350	-360	-380
RNC5		-385		-328	-295	-127	-260	-710	-343	-389
RNC6		-242	-228							
RNC7		-472	-462							
RNC8		-250		-314	-230	-250	-314	-284	-220	-326

NOTES

- First letter of specimen name corresponds to cylinders [C] or beams [R]. If second letter is "N" there are no built in chlorides. Italicized rows indicate specimens discussed in this report. Highlighted specimens have been removed from the tank and have been autopsied.
- Half-cell readings from 2/99 are reported in 1774-2.

TABLE A-3 RESULTS OF AUTOPSIED SPECIMENS

Specimen (a)	Autopsied Specimens Results [c]			
	Average chlorides (%)		Average half cell (mV)	
	Unwrapped	Wrapped	Unwrapped	Wrapped
CC1				
CC2				
CC3		0.085		-225
CC4				
CC5		0.200		-460
CC6		0.150		-460
CC7		0.220		-610
CC8				
CC9				
CC10	0.337		-454	
CC11	0.290		-517	
CC12				
CC14				
CC15	0.214	0.103	-477	-391
CC16				
CC17	0.426		-534	
CC18	0.440		-590	
CC19				
CC20				
CC21				
CNC1				
CNC2				
CNC3				
CNC4				
CNC6	0.352	0.053	-561	-401
CNC7				
CNC8		0.170		-410
CNC9				
CNC10		0.003		-350
CNC11	0.318		-463	
CNC13		0.120		-600
CNC14		0.020		-540
CNC15				
CNC16	0.070	0.007	-515	-189
CNC17	0.120	0.001	-536	-94
CNC18				
CNC19		0.130		-560
CNC20	0.414		-554	
RC1				
RC3	0.080	0.082	-454	-315
RC4		0.350		-610
RC5	0.282	0.047	-438	-260
RC6				
RC7		0.120		-680
RC8				
RC9				
RNC1	0.184	0.001	-505	-339
RNC2	0.125		-412	
RNC4				
RNC5				
RNC6		0.002		-230
RNC7		0.210		-470
RNC8				

NOTES

- First letter of specimen name corresponds to cylinders [C] or beams [R]. If second letter is "N" there are no built in chlorides
- Highlighted specimens are those that have been removed from the tank and have been autopsied
- Readings are averaged in the appropriate wrapped and unwrapped portions of the autopsied specimens (R)
- Chloride contents in bold numbers are below threshold values. 64

Table A-4 CHARACTERISTICS AND CHRONOLOGICAL RECORD OF HALF-CELL READINGS OF SPECIMENS WITH DIFFERENT CORROSION INHIBITORS

Specimen	Wrap	Crack. Condition	Corrosion Inhibitor	Half-Cell Readings in Tank (mV)						
				2/15/2002	3/5/2002	1/10/2003	2/10/2003	12/4/2003	12/16/2003	27/04/2003
1	delta-24"	Cracked	Surtreat	-308	-217	-339	-317	-420	-413	-450
2	delta-36"	Cracked	Surtreat	-269	-180	-272	-278	-420	-420	-461
3	delta-24"	Uncracked	Surtreat	-283	-212	-308	-260	-320	-266	-330
4	delta-36"	Uncracked	Surtreat	-351	-345	-332	-335	-400	-395	-443
5	delta-24"	Cracked	Cortec	-363	-284	-424	-412	-460	-434	-489
6	delta-36"	Cracked	Cortec	-291	-284	-333	-338	-430	-371	
7	delta-24"	Uncracked	Cortec	-267	-252	-346	-320	-350	-348	-403
8	delta-36"	Uncracked	Cortec	-389	-355	-373	-365	-430	-382	-452
9	delta-24"	Cracked	Sika	-325	-271	-335	-283	-400	-386	
10	delta-36"	Cracked	Sika	-261	-184	-329	-331	-460	-337	-473
11	delta-24"	Uncracked	Sika	-321	-317	-287	-262	-555	-485	-506
12	delta-36"	Uncracked	Sika	-345	-415	-352	-345	-430	-374	-508
13	delta-24"	Cracked	None	-230	-183	-261	-242	-280	-275	-324
14	delta-36"	Cracked	None	-270	-253	-280	-262	-320	-5	-385
15	delta-24"	Uncracked	None	-287	-219	-253	-247	-350	-240	-342
16	delta-36"	Uncracked	None	-324	-305	-326	-327	-365	-356	-409
19	none	Cracked	None	-536	-428	-527	-442	-410	-3	-510